OPTIMIZATION, FORMULATION AND EVALUATION OF β-CAROTENE AND β-GLUCAN ENRICHED PASTA WITH PUMPKIN AND OAT FLOUR

Sinthiya R[1], Dr.A.Lovelin Jerald[2] , Veerapandi Loganathan[3]
[1]Research Scholar, Department of Food Technology, School of Engineering, Avinashilingam Institute for Home Science and Higher Education for Women, Avinashilingam University, Coimbatore (India).
[2] Department of Food Technology, School of Engineering, Avinashilingam Institute for Home Science and Higher Education for Women, Avinashilingam University, Coimbatore (India).
[3]Department of Food Technology, Nehru Institute of Technology, Kaliyapuram, Coimbatore, Tamil Nadu, 641105, India.
*Corresponding Author: Sinthiya R, Research Scholar, Department of Food Technology, School of Engineering, Avinashilingam Institute for Home Science and Higher Education for Women, Avinashilingam University, Coimbatore (India).

Abstract
This study explores the formulation and quality assessment of pasta enriched with pumpkin and oat flours, aiming to enhance its nutritional and functional characteristics Utilizing a response surface methodology (RSM), with 10-15% pumpkin flour and 75-85% oat flour. This composition notably increased β-carotene and β-glucan content, as well as fiber, improved heart health and reduced risk of chronic diseases. The enriched pasta exhibited altered cooking qualities, with reduced cooking time and cooking losses. Sensory evaluations revealed favorable consumer acceptance, especially with formulations containing 10% pumpkin flour, which maintained desirable taste and texture. While higher concentrations of pumpkin flour enriched the pasta's nutritional profile, sensory attributes. Microbiological analysis indicated that the product could be safely stored under refrigeration for up to 45 days. The findings suggest that incorporating pumpkin and oat flours can create functional pasta with enhanced health benefits, recommended to balance nutritional and sensory attributes for commercial viability.

Keywords: Pasta, β-Carotene, β-Glucan, response surface methodology, Fortified pasta.

Introduction
Functional food is part of the fastest growing sector in the global food market and a response to the growing consumer demand for health products(Kim et al. 2012). According to the European Commission, the term "functional food" refers to food that, aside from its nutritional effects, exerts a beneficial effect on the physical functions of the body and, in some cases, reduces the risk of particular diseases (Javeria et al. 2013). These beneficial results must be scientifically verified. Functional food must be available in a form that is accessible to consumers within the daily diet. A diet that is unevenly balanced places a great burden on developing chronic NCD. There is still a rising trend for type 2 diabetes and cardiovascular diseases (Braaten et al. 1994a; 1994b). An integral part of preventing these diseases is to increase dietary fiber intake (Hooda et al. 2010). Several studies have emphasized that high consumption of cereal-derived fiber is associated with a reduction in the risk of development of type 2 diabetes (Drozdowski et al. 2010). Dietary fiber has been used for fortification for many years. Its soluble fractions (SDF) are thought to be extremely functional. During the last decades, many clinical researches demonstrated the positive impact of the soluble β-glucans fibers not only on the blood cholesterol level (Bae et al. 2010), but also on the postprandial blood glucose level and insulinemic response (Wood, Beer, and Butler 2000). Pasta is one of the most popular products made from durum wheat grain or semi-grain. They generally have low glycemic index and durability(Pongjanta et al. 2006). Enrichment of pasta with functional

ingredients of a higher biological value is an ideal product for enrichment. Pumpkin flour is a promising raw material for enriching flour products with valuable nutrients (Kwiri et al. 2014). It is also known that pumpkin flour contains 6.1 % of water, 8.2 % of protein, 0.7 % of fat, 2.3 % of ash, 27.4 % of dietary fiber, which consists of 10.2 % soluble and 17.2 % of insoluble fibre. The introduction of pumpkin flour into dough altered its farinographic characteristics, (Hussain et al. 2021)water absorption and time for the dough formation increased, whereas stability of dough and the index of resistance to kneading decreased. In addition, enrichment of flour products with pumpkin flour influences the technological parameters of the final product. Thus, bakery products acquired a smaller volume and specific volume. Replacement of wheat flour with pumpkin flour by more than 5% assisted in reducing the product bulge and enhancing the hardness of the latter during storage. The enrichment of foodstuffs with pumpkin flour also affects its sensory properties (Nkhata and Ayua 2018). Pasta and pumpkin flour are used in the technology of enriched products with pumpkin-containing semi-finished products. The use of pumpkin seed flour is very popular]. Much less is used of fresh pumpkin pulp (puree, straws of various shapes and sizes, slices, etc.) (Carvalho et al. 2014). The use of pumpkin flour has some advantages compared with other pumpkin processing products. The main advantage of pumpkin flour is the possibility of longer storage as compared to fresh pumpkin(Norshazila, Rashidi, and Irwandi 2014). In addition, the share of fruit and vegetable flour in the product recipe is much smaller, compared to moisture-containing semifinished products. Thus, in work(Nakazibwe, Olet, and Rugunda 2020), the replacement of 25 % of corn flour with pumpkin flour in the pasta's recipe gave a positive effect on the color and texture. At the same time, the addition of 25 % of pumpkin flour demonstrated the maximum sensory evaluation by consumers. For 50 % pumpkin flour, the organoleptic evaluation of pasta deteriorated, but according to the study(Amin et al. 2019), 10 % pumpkin flour added to the recipe of pasta proved to be optimal, because the highest sensory evaluation was brought, therefore the color, aroma, taste and consistency of the pasta got 8.2–8.8 points. Meanwhile, the content of beta-carotene in pasta significantly increased by applying 5–20 % of pumpkin flour. It has to be mentioned that the high organoleptic evaluation belonged to the pasta whose recipe contained 20 % of wheat flour substituted with pumpkin flour (Kreck et al. 2006). However, in such experiments, the options of experiment had a big interval and it is impossible to establish optimal amount of pumpkin flour. That is necessary, since the obtaining technology of pumpkin flour is significantly different from the one of wheat flour production. At the same time, the addition of pumpkin flour significantly increases cooking losses, as noted in (Cheng and Lai 2000). The most significant losses occurred at the stage of cooking added 10 % pumpkin flour, which is equivalent to 6.6%. Simultaneously, the introduction of pumpkin flour into a recipe worsened sensory evaluation of pasta using response surface methodology. Pasta enriched with beta-carotene, beta glucan, and physical properties were added by pumpkin flour. The correct amount of pumpkin flour in pasta varies widely in the literature, from 5 to 15 %. In addition, the smell and taste of the pumpkin component in pasta after cooking undergo sensory evaluation. The level of sweet taste of pasta with the addition of pumpkin flour was not analyzed. Thus, scientific research on the rational use of pumpkin flour in pasta is needed for its utilization.

Materials and methods

Raw materials

Experimental stage of the research was carried out at laboratory of the Department of Food Technologies of Avinashilingam university, Coimbatore, India. For this work, oats were used with the moisture content in flour 10%. Pumpkin flour with the moisture content of 13% was produced from pulp of large-fruited pumpkin (*Curcubirta Pepo*.) India. Pumpkin processing technology included such stages as cleaning, grinding into smaller particles size

500±20×1.5±0.5 mm. Drying was conducted in a cabinet tray dryer at 60±3°C to constant mass. After drying, the pulp was crushed in a KR-20S hammer crusher (China) and sieved on a sieve.

Pasta Preparation

The pumpkin flour, oat flour and water are added together to the mixing chamber. The pasta dough which has been mixed up, moulded, but not at standard can also be added to the mixing chamber. In order to prevent dead parts in the dough that causes stagnation and fermentation, the tank usually has a cylinder-like shape. The tank cover is a very important item it should be designed so that it can be observed through; in this way, it is possible to sight into the preparation of the dough. The dough is thoroughly mixed by two opposed shafts working in the direction of counterrotation; these mixers are designed to provide the minimum amount of lumping or balling. The rotary shafts carry some blades mounted in a propeller-like arrangement; the blades at the ends of the shaft act like scrapers to clean the front walls. The activity of the blades, the dough mass and time for operation have to be such that will achieve the uniform hydration of the flour. This mixture is mixed until it makes a stiff dough which when squeezed with one's hands hold together as a solid lump. When water first added to the flour, then its compact tight structure is soon lost. It absorbs the water and swells too much over an open structure. The mixing should just wet the flour and not destroy the structure (Suknark et al. 2001). Temperatures during mixing are not high, not higher than 55ºC, therefore neither partial formation of gluten network would occur due to gliadin and glutenin denaturation. Also if dough reaches the temperatures within 60-70 ºC the gluten loses its ability to extend due to its thermic coagulation along with albumins and globulins.

The formulation applied to all fresh pastas prepared here is given in table 1. Specifically, the sample coded was a reference standard fresh pasta made with oats and pumpkin flour. All samples were extruded through a single screw extruder; the dough is kneaded by the shearing of the rotating screw. The dough and the machinery soon become hot if the extruder barrel were not kept cooled at around 45ºC (Kris-Etherton, Harris, and Appel 2002). The barrel and the die temperature is therefore maintained at around 45ºC by circulation of cold water at temperature around 19-25ºC and the extrusion is best carried out at intermediate speeds (30 rpm). Extruded pasta cut by rotated knives shave off outer surface of the die, the more rapidly the knife rotates, the smaller the pasta pieces become; the rotation speed of the knife is set to a constant; this way, spurious variations in the flow of extruded dough need to be avoided; pasta thus obtained was dried and kept for further analysis.

Estimation of *β*-Carotene

β-Carotene extraction was carried out according to the procedure described by (Barba et al. 2006a) with slight modifications. β-Carotene was extracted by soaking sample 0.5 g in water at room temperature kept under dark condition for complete extraction. The suspension was stirred magnetically for 30 min. The extracts were centrifuged to separate the supernatant, and these operations were repeated until the pasta was completely colorless. The extracting solvents were made up to 50 mL in volume. Finally, the absorbs of the extracts were evaluated using UV spectroscopy methods.(Karnjanawipagul et al. 2010)

Proximate Analysis of Pasta

Moisture Analysis

The moisture content was determined by the AOAC method (Agroindustriais 2013). Moisture content of the pasta samples was analyzed using an MX-50 Moisture Analyzer. 1 g sample was evenly on the heating pan and temperature is set at 140ºC for 5.8 mins.

$$Moisture\ content = \frac{wt.of\ the\ original\ sample - wt.of\ the\ dried\ sample}{wt.of\ the\ original\ sample}$$

Dietary Fibre (%)
Sample free from moisture and fat was hydrolysed with amyloglucosidase and protease in order to remove starch and proteins. The supernatant was precipitated with 78 percent ethanol for the precipitation of soluble and insoluble fibers that were separated by filtration. The residue that remained from the filtration was washed by ethanol and acetone followed by oven drying, weighing, and ignition to ash (Asp et al. 1983).

Ash Content
Five grams of ground pasta was taken in a previously weighed silica crucible and contents were evaporated over a water bath. On drying, the contents were ignited over a hot plate. On dry mass charring, the crucible was placed inside an electric muffle furnace at 500°C and contents allowed to ash completely. The crucible was taken out after it had been completely ashed, and it was cooled in a desiccator and weighed very cautiously with the help of a chemical balance. The ash contents of pasta were computed as follows ((Hussain et al. 2021)).

Empty weight of silica crucible = W1g

Weight of silica crucible + ash = W2g

Weight of ash alone = (W2-W1)g

Percentage ash = $\frac{W2-W1}{5} * 100$

Resistant Starch Determination
The starch was isolated from the flour using a procedure suggested by (Cheng and Lai 2000) and the drying of the starch was done at 50°C in a cabinet drier. This was done by extracting 50gm of the meal twice with 500ml of distilled water, suspending the precipitated starch in water and allowing it to settle for 24hours at 4°C. The supernatant was then siphoned off and the residue was dried at 50C in a cabinet drier. The starch cakes were then powdered in a Waring blender and passed through a sieve of size 250.

Optimum Cooking Time (OCT)
Then, spaghetti strands weighing 20 g are cut into equal size of 100 mm and boiled in 300 ml boiling water. During its cooking, optimum cooking time was estimated at an interval of every 30 s by the disappearance of white core of spaghetti through squeezing between two transparent glass slides based on the AOAC Approved Methods of Analysis, Method 66-50, 2000. The time when the white core completely disappeared was the optimum cooking time, OCT (AOAC 2000).

Cooking Loss (CL)
The content of solid matter lost into the cooking water was assessed through use of (AOAC Approved Methods of Analysis, Method 66-50, 2000). Ten grams of spaghetti was cooked with 300 ml of boiling water at OCT. The above was rinsed with 100 ml of cold water, and then trained for 30 s to determine the cooking loss of the pasta. The cooking water was collected in an aluminium vessel, kept in the air oven at 105° C, to evaporate the water until a constant weight was obtained. The residue was weighed and the percentage of the starting material was reported. The above analysis was performed in triplicate.

Swelling Index (SI)
The swelling index of cooked pasta was determined as described before. Ten grams of spaghetti was cooked in a closed tube with boiling water at 5 ± 1°C at OCT (Biswas, Sahoo, and Chatli 2011). It was then rinsed with 100 ml cold water. The diameter of spaghetti strands was measured before and after cooking, and the swelling index was determined based on the

following equation: SI=D2−D1D1×100where: SI: Swilling Index, D1: Diameter before cooking, D2: Diameter after cooking (AOAC 2000).

Microbiological Analysis

Total plate Count

Bacterial count from pasta sample was determined by employing nutrient broth as the medium. Sample 1ml were diluted serially from 101 to 104 peptone water (0.1%), 0.1 ml samples from appropriate dilutions were spread plated onto agar plates. Enumeration for viable cells was performed in duplicate, incubated at 30°C for 48-72 hours. Viable cell count is the average of two separate dilutions for each sample (De Nardo et al. 2009).

Total Coliform

Brilliant Green Lactose Bile Broth 2% has been used for the isolation, differentiation, and enumeration of coli form bacteria. It is made by American Public health Association. It contains two inhibitors of both gram positive and selected gram-negative organism i.e., ox gall and brilliant green dye. Pasta samples (1ml) were serially diluted from 101 to 104 in peptone water (0.1%) and 0.1 ml of the samples from the appropriate dilutions were spread plated onto malt extract agar. Viable cells count, performed in duplicate, was determined after 5days incubation at 25°C.for every sample two separate dilutions were enumerated and averaged for the viable cell count(Baranska, Schütze, and Schulz 2006).

Sensory Evaluation

Traditionally, sensory evaluation has been defined as the scientific application of evoking, measuring, analyzing and interpreting those responses to products as perceived by the human senses: sight, smell, touch, taste and hearing (Abrha et al. 2016). They can be broadly classified into two areas: objective testing-analytic, and subjective testing-hedonic. In objective testing, sensory attributes of a product are assessed by a panel selected and trained. It measures the reactions of consumers toward the sensory attributes of products under subjective testing. The scale used for sensory evaluation is as given below.

Scale:

Like extremely	: 9
Like very much	: 8
Like moderately	: 7
Like slightly	: 6
Neither like nor dislike	: 5
Dislike slightly	: 4
Dislike moderately	: 3
Dislike very much	: 2
Dislike extremely	: 1

Experimental Design

By the application of statistical discovery software from (11.0.5.0 version, Stat-Ease Inc.), the optimum formulation of pumpkin-oats pasta can be determined by RSM. The optimum formula of the pumpkin-oats pasta can be obtained using the application of the Box-Behnken design in RSM. The effects of two independent variables listed in Table 1, namely pumpkin flour and oats flour have been coded as A and B respectively. The above and below limits for the independent variables were set. The beta-carotene, betaglucan, moisture, ash, fiber, sugar, resistant starch was selected as response variables. Design of Box-Behnken response surface analysis is showed in table 2. There was total 12 randomized experiments. Five replications at the center point where each coded variable 0 was run to establish the repeatability of the method for good experimental results (Careri, Elviri, and Mangia 1999).

Interaction and effects of two factors on response variables were studied with the polynomial regression equation. From the result of ANOVA, the experimental data of response variables were fitted into the polynomial regression model. The proposed model was enumerated in the following equation:

$$\eta = \beta_0 + \beta_1 x_1 + \beta_2 x_2 + \beta_{12} x_1 x_2 + \beta_1 x1^2 + \beta_2 x_2^2$$

The optimum formulation of pumpkin-oats pasta recipe was calculated using a multiple response method named desirability that ranges from 0 (undesirable) to 1 (very desirable). Response surface plot was generated, which is a helpful tool for better understanding of the relationships of each factor and response, and it will display in a three-dimensional view (Rungpichayapichet et al. 2015).

Table 1: Ranges of independent variables used for making model

Independent variables	Unit	Levels	
Pumpkin Flour, X_1	%	5	15
Oats Flour, X_2		75	85

PHARMACOLOGICAL PROPERTIES ANALYSIS

PROTEIN DATA BANK

The Protein Data Bank (PDB) database is a single global repository of information on the 3D structure of large biomolecules, including proteins and nucleic acids. They are molecules of life found in all living things, including bacteria, yeast, plants, flies, other animals, and humans. It helps to understand the shape of a molecule infer the role of structure in human health and disease and in drug development. Structures in the database range from small proteins and fragments of DNA to complex molecular machines such as ribosomes. The three-dimensional structure of Wild-Type Human Pancreatic Alpha-Amylase (*4X9Y),* Human Aldose Reductase in complex with ALR25 *(6TUC)* were retrieved from the Protein Data Bank.

PUBCHEM

PubChem is an open chemistry database at the National Institutes of Health (NIH). It is a collection of information on chemical structure, identification, chemical and physical properties, biological activity, patents, health, safety, toxicity data and much more. PubChem mainly contains small molecules but also larger molecules such as chemical compounds including drugs, nucleotides including siRNA and miRNAs, carbohydrates, lipids, peptides, chemically modified macromolecules. The canonical smile of the ligands was extracted from the PubChem database.

ACTIVE SITE IDENTIFICATION:

CASTp (sts.bioe.uic.edu/castp/index.html?201|) server is used for identification of probable active sites.

SWISSADME:

The SWISSADME server was used to analyze the molecular structure of the ligand, confirming that the ligand uses five (or) steps of the Lipinski rule. Lipinski's Rule of Five provides guidance on the solubility, bioavailability, and permeability of the drug molecule of interest. The drug-likeness properties of 30 compounds were extracted from this server.

ADME/T-SAR:

Pharmacological properties were predicted using ADME/T- SAR which is an inline-based tool that includes the AMES toxicity, human abdominal adsorption etc. The ADME/T properties of the 30 compounds were retrieved from this server for further studies.

AUTODOCK 4.2:
Protein-ligand binding studies were performed using the AutoDock4.2 program. It is one of the most widely used methods for protein-ligand binding. Docking analysis of Wild-Type Human Pancreatic Alpha-Amylase *4X9Y &* Human Aldose Reductase in complex with ALR25 *(6TUC)* were performed separately for beta-sitosterol, 9,12-octadecadienoic acid (Z, Z) and n-hexadecenoic acid.

VISUALIZATION:
The docked files are visualized using Pymol, Maestro, Chimera, PDBsum, PLIP and protein plus.

Results And Discussions
One of the important stages of scientific investigation is the choice of a method for the statistical processing of information which ensures that an error is made in the least possible degree. The choice of a method of statistical processing depends on the kind of distribution of the data (Abdullah et al. 2020). The highest value of the boiling coefficient by volume (1.85) was in the control sample. Increasing the amount of pumpkin flour decreased this indicator. Such a property was defined by the properties of pumpkin flour, water absorption capacity of which is significantly different from the one of semi-grain. The other important point in the composition of pumpkin flour is the lack of gluten, which preserves pasta shape when being cooked. Evidently, pasta with pumpkin flour addition lost more mass when being cooked. Pumpkin flour is powerfully flavored and aromatic, which most likely negatively affects the food quality of the ready-made product from the perspective of each individual consumer. Thus, in developing the pasta recipe, the main requirement was to create a product with high indicators of sensory quality. The main criteria for the organoleptic evaluation of pasta products enriched with non-traditional raw materials are smell and taste. From the consumer's point of view, the smell of pasta significantly decreased with an increase in the amount of pumpkin flour (Fig. 3, a). A further increase in the amount of pumpkin flour to 15 % led to a less significant, but reliable decrease in the smell evaluation from the consumer's point of view by 0.2–0.4 points. The tendency to shift the taste of pasta on the concentration of pumpkin flour was close to transforming the smell (Fig. 3, b). The experiment proved that consumer evaluation, when pumpkin flour was added from 5 to 7.5 %, resulted in a product with high taste indicators – 8.9-9.0 points, close to the control version. The more the pumpkin flour used the more reduced the taste of the obtained products (Chen et al. 2016; Petracci et al. 2014; Prasetyo et al. 2008). The lowest rating of taste from the consumer's point of view was achieved with the addition of 15% pumpkin flour. According to the assessment of sensory evaluation, it can be said that the incorporation of pumpkin flour significantly altered the smell of pasta the most. At the same time, the taste of pasta remained at a high level. This is explained by the fact that pumpkin flour contains aromatic substances in its composition, which carry its flavor to the end product. Identification of such substances and further work on their minimization are important tasks. The influence of non-traditional components in the technology of product on sensory indicators has been proved(Rungpichayapichet et al. 2015).

Table 2: Model with independent variables

Sl No:	Run	Pumpkin %	Maida %
1	11	2.92893	80
2	2	5	75
3	5	5	85
4	10	10	72.9289
5	13	10	80
6	1	10	80
7	9	10	80
8	6	10	80
9	12	10	80
10	8	10	87.0711
11	4	15	75
12	7	15	85
13	3	17.0711	80

Beta-carotene:

As evident from Table 3&4, independent parameters of pumpkin flour (X1) ($P < 0.001$) and another independent variable oat flour (X2) had a significance towards the Beta-carotene. Its combination terms X1X2 had a negative effect whereas quadratic terms X12, and X22 ($p < 0.05$) also had a negative effect in Figure 1. The R2 of regression was at a value of 0.9542, and the result showed that the regression model had explained the variability of data to the extent of about 95%. While researching on the processing of extruded food incorporated with pumpkin flour, it is shown that a similar effect occurred according to (Ganesan et al., 2017). The equation indicates the model with coded terms:

Beta-carotene = $388.20 + 38.40X_1 + 5.29X_2 - 0.75X_1X_2 - 9.29X_1^2 - 7.79X_2^2$ ……. (7)

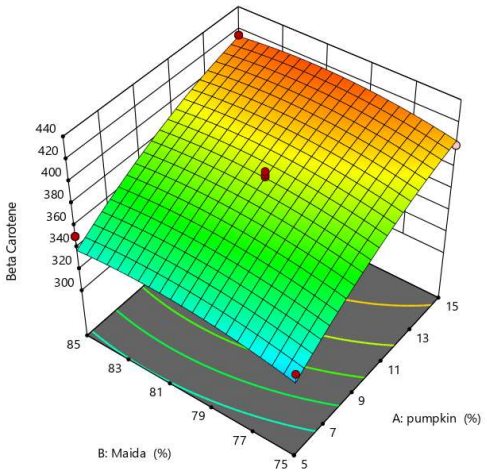

Figure 1: The effect of independent variables on beta-carotene

Table 3: The regression coefficients, AAD, MSE. MPE, RSME, R^2, adjusted R^2, and predicted R^2 of the responses

Coefficients	Beta Carotene	Beta Glucan	Moisture	Ash	Fiber	R Starch	Sugar
X_0	+388.20	+20.00	+3.69	+0.0782	+2.32	+2.48	+3.35
X_1	+38.40****	+4.41****	-0.796****	+0.0706****	+0.2629****	+0.7654****	-0.9458****
X_2	+5.29	+0.3643	-0.0662	+0.0166*	+0.5169*	+0.1588*	-0.0091
X_{12}	-0.7500	-0.1250	-0.2797*	+0.0146	-0.3487*	+0.0260	+0.0445
X_{11}	-9.29*	-1.22*	-0.2046*	+0.0207*	+0.4179*	-0.1761*	+0.0458
X_{22}	-7.79	-0.9687*	-0.0166	-0.0048	+0.0767	-0.0303	-0.3639*
R^2	0.9542	0.9590	0.9610	0.9669	0.9173	0.9732	0.9296
Adj. R^2	0.9214	0.9298	0.9331	0.9433	0.8583	0.9541	0.8793
Pred. R^2	0.7146	0.7860	0.7854	0.7686	0.6925	0.8612	0.7600
Lack of Fit	not significant	not significant	not significant	not significant	not significant	not significant	not significant

Beta-Glucan

From Table 3&4, it is quite evidently showing that Beta-Glucan was significantly positive by pumpkin flour (X1) oat flour (X2) and the other terms are like independent term X2, interaction term X1X2, and quadratic terms are X12, X22 ($P<0.001$) has linear negative result. And hence from the above-mentioned equation, the R2 value was attained as 0.9590. Thus, the model indicates 95% possibility for getting Beta-Glucan while using this combination. Figure 2 also depicts that Beta-Glucan content increased. However, Beta-Glucan content has exhibited a very highly positively significant effect for all other combinations (Norshazila, Rashidi, and Irwandi 2014). The coded equation for this mentioned term is given below regression model with coded terms:

$$\textbf{Beta-Glucan} = 20 + 4.41X_1 + 0.364X_2 - 0.125X_1X_2 - 1.225X_1^2 + 0.968X_2^2 \quad \textbf{(8)}$$

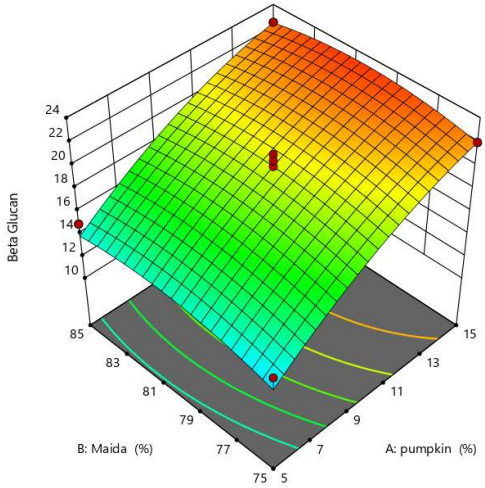

Figure 2: The effect of independent variables on beta-Glucan

Moisture content:

From table 3&4, the all-independent variable, combination of X1X2, quadratic term X12 (P<0.01) and another quadratic term X22 had a linear negative result on moisture content. The R2 value 0.9610 was obtained from the above equation which shows that the model has examined up to 96% significant to getting a better texture. Similarly, figure 3 shows the effect of independent variables in moisture content. Figure 3 defines that moisture content was influenced by independent variables. The regression equation for the moisture content of pasta is given in coded forms:

Moisture content = $3.69 - 0.792X_1 - 0.0662X_2 - 0.279X_1X_2 – 0.204X_1^2 - 0.016X_2^2$ ……. (9)

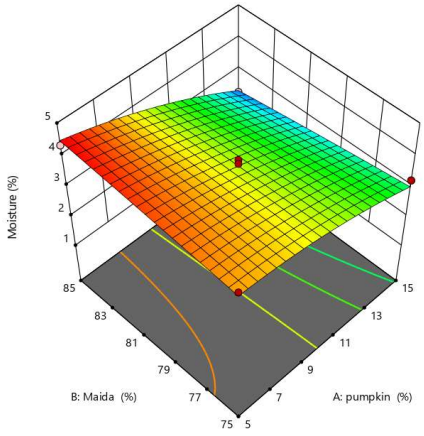

Figure 3: The effect of independent variables on moisture content

Ash Content:

Independent variables, combined variables X1X2, quadratic term X12 (P<0.01) and X22 of pasta along with the relation is presented in table 3&4. Obviously, it depicts that ash content of pasta had positive effects from independent variables, combined variables X1X2, quadratic term X12 (P<0.01) and X22 had negative impacts shown in Figure 4. The R2 value of ash content was 0.9433 achieved from the above equation. It further indicates that this model can describe 94% data variability. The following equation was seen describing the role of ash content along with its independent parameters and coded term:

Ash Content = $0.0782 – 0.0706X_1 + 0.0.0166X_2 + 0.0146X1X_2 + 0.0207X_1^2 - 0.0048X_2^2$ …… (10)

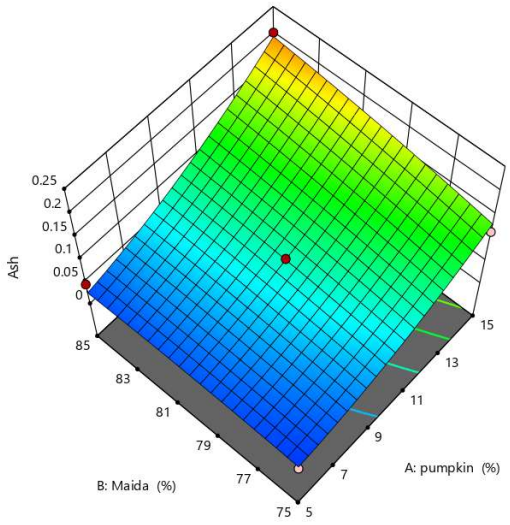

Figure 4: The effect of independent variables on Ash content

Fiber Content:

Table 3&4 was presented as the mathematical representation of protein content. From the table 3&4, it remains well evident that all the parameters X1 (P<0.001), X2 (P<0.001) and quadratic term X12, X22 (P<0.001) are at highly significant except the combined variable X1X2 had a linear negative effect on fiber content of pasta. This regression equation evidently states that this model is appropriate for protein content experimental results, an R2 value 0.9173 was obtained meaning the model explains 91% of the variance of response. Also, in figure 5 the effect of fiber content of pasta was shown, it was observed from the response surface graph between fibre content and independent variables. Quadratic model achieved for the coded terms of variables of pasta regression analysis as follows:

Fiber Content = $2.32 + 0.262 + 0.516 - 0.348X_1X_2 + 0.417X_1^2 + 0.0767X_2^2$ ……. (11)

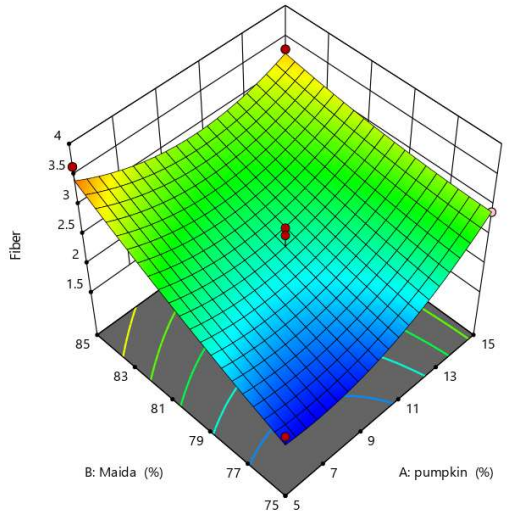

Figure 5: The effect of independent variables on fibre content

Resistant Starch:

According to the coefficient table 3&4, the content of Resistant Starch was significant positive due to pumpkin flour X1 (P<0.01), independent term tomato pulp X2, interaction term X1X2 had also linear positive result on pasta. quadratic terms are X12 (P<0.5), X22 also had a negative result on pasta. The obtained value of regression model has a 0.9732 R2, showing up

to a 97% variance of data. From Figure 6 plot, it was studied that those factors which positively affected the Resistant Starch of pasta. In coded planes, regression equation was developed for the effect of independent variables on Resistant Starch content of pasta is given below:

Resistant Starch = $2.48 + 0.765X_1 + 0.158X_2 + 0.026X_1X_2 - 0.176X_1^2 - 0.030X_2^2$ …… (12)

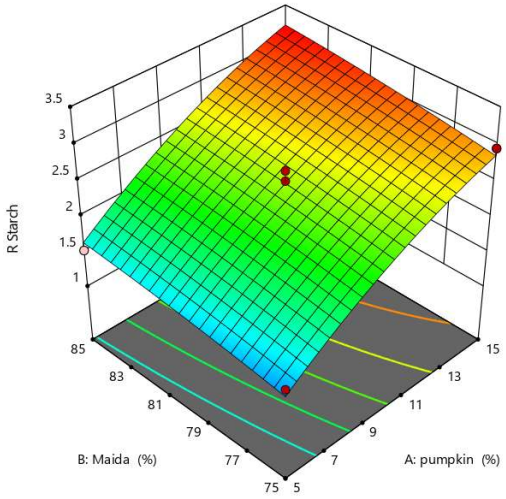

Figure 6: The effect of independent variables on fibre content

Table 4: Box-Behnken Design: Experimental and predicted values of responses at different experimental conditions for RSM and ANN

Sl No:	Pumpkin %	Maida %	Beta Carotene		Beta Glucan		Moisture		Ash		Fiber		R Starch		Sugar	
			Exp	Pred	Exp	Pred	Exp	Pred	Exp	Pred	Exp	Pred	Exp	Pred	Exp	Pred
1	10	80	386.00	388.20	21.00	20.00	3.59	3.69	0.0812	0.0782	2.17	2.32	2.51	2.48	3.65	3.35
2	5	75	335.00	326.69	14.00	12.91	4.17	4.05	0.0167	0.0214	1.85	1.69	1.48	1.38	4.29	4.03
3	17.0711	80	428.00	423.93	24.00	23.80	2.05	2.15	0.2270	0.2195	3.53	3.53	3.22	3.21	2.23	2.11
4	15	75	401.00	404.98	22.00	21.99	3.22	3.01	0.1163	0.1336	2.91	2.91	2.95	2.86	2.05	2.05
5	5	85	352.00	338.77	15.00	13.89	4.33	4.47	0.0455	0.0255	3.64	3.42	1.53	1.64	4.04	3.93
6	10	80	391.00	388.20	20.50	20.00	3.75	3.69	0.0799	0.0782	2.05	2.32	2.65	2.48	3.70	3.35
7	15	85	415.00	414.06	22.50	22.46	2.27	2.32	0.2033	0.1959	3.31	3.25	3.11	3.23	1.98	2.12
8	10	87.0711	372.00	380.11	18.00	18.58	3.71	3.56	0.0733	0.0921	3.05	3.21	2.81	2.65	2.66	2.61
9	10	80	381.00	388.20	19.00	20.00	3.88	3.69	0.0794	0.0782	2.64	2.32	2.44	2.48	3.06	3.35

10	10	72.9289	364.00	365.14	17.00	17.55	3.53	3.75	0.0613	0.0452	1.68	1.75	2.05	2.20	2.48	2.64
11	2.92893	80	302.00	315.32	10.00	11.32	4.43	4.40	0.0094	0.0196	2.57	2.79	1.05	1.05	4.54	4.78
12	10	80	394.00	388.20	19.50	20.00	3.56	3.69	0.0743	0.0782	2.52	2.32	2.46	2.48	3.01	3.35
13	10	80	389.00	388.20	20.00	20.00	3.65	3.69	0.0761	0.0782	2.24	2.32	2.35	2.48	3.34	3.35

Sugar:

In this study, independent parameter X1 ($P<0.001$), X2 and quadratic term X22 was also strong positive parameters while independent term X2, interaction parameter X1X2 and quadratic term X22 had a positive result. All model terms were of positive effect which are given in Table 3&4, while interpreting R2 the pasta value was 0.9296. Also, (Quijano-Ortega et al. 2020)specifies that the ratio of these two is more than 4 is desirable. Also, the model indicates that variance 92% for data and the response has shown exceptional interaction between the trial and predicted value. The Figure 7 have shown that the quadratic model was satisfactory in assuming the response variables for the experimental data. The quadratic equation was obtained by using the Box-Behnken design, and the experimental interaction between the independent variables and different responses in coded terms were provided based on trial results as follows.

$$\textbf{Sugar} = 3.35 - 0.948X_1 - 0.0091X_2 + 0.044X_1X_2 + 0.045X_1^2 - 0.363X_2^2 \ldots\ldots \textbf{(13)}$$

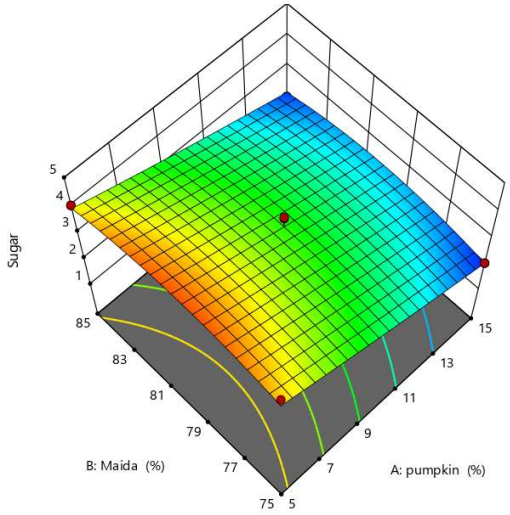

Figure 7: The effect of independent variables on fibre content

Optimum cooking time of pasta

The optimum cooking time (OCT) of pumpkin flour fortified pasta is 13.00 ±1.30. As indicated, there is a reduction in cooking time as the concentration of pumpkin flour increased compared to the control. The control had an OCT of 20 mins while for pumpkin flour fortified pasta it ranged from 10-15 min. These findings are in agreement with that of (Norshazila, Rashidi, and Irwandi 2014) who established the same trend using fortified chickpea flour spaghetti. The outcome cooking times reduction might be attributed to the high rate of water diffusion to the core of pasta within the lack of continuity in the protein-starch network that could have allowed the water diffusion through the pasta matrix, leading to a diminished time for water to penetrate into the centre during cooking, as stated by (Pritwani and Mathur 2017a).

Cooking loss

The solubility of nutrients in water caused losses as it was absorbed by pasta during cooking, leaving the mass fractions of the nutrients to decrease. All the obtained cooking loss values are within the acceptable limits since the loss of solids in cooking water should not exceed 9%, according to (AACC Approved Methods of Analysis, Method 66-50, 2000). The cooking loss presented a drastic gradual reduction along with the pumpkin flour concentrations that reached the minimum value (11.1±0.4), 4.02% as compared to the control value, 4.64%. This is supported by (Nisa and Walanda 2021) who also recorded the same trend with fortified spaghetti of common bean. These results could be said to belong to the network of protein-starch, where increased protein content was stated to hinder gluten development and weaken the structure which allows the loss of more solids (Aremu and Nweze 2017). Due to different protein and carbohydrate contents in formulation, starch-protein new arrangements have been reported (Zahra et al. 2016). Fortification of pasta with chickpea and quinoa flour was reported to reduce cooking time, increase cooking lose, as well as having effects on firmness and cohesiveness (Moh et al. 1999).

Swelling index (SI)

The swelling index was expressed in terms of the cooking quality of pumpkin flour fortified pasta. Compared to the control, swelling index (SI) values were drastically increased in samples added with pumpkin flour and had a direct proportional relation with increased concentration. The results obtained can be explained in reference to the water absorption behavior of pumpkin flour, where legume proteins were reported to have high water absorption capacities (Barba et al. 2006b). These results are consistent with (Moh et al. 1999)who reported that more dense fine particle size enhances the uptake of water and volume expansion of pasta, thus having higher hydratability capacity.

Sensory evaluation

Sensory evaluation of pasta fortified with pumpkin flour was performed compared to control. Despite that pasta fortified with pumpkin flour, sensory parameters showed to be comparable to control, but P6 showed to be more preferred to panelists (Fig. 3A, B). These results can be ascribed to lower starch content that is significantly pronounced both in treatments that reflected as better quality and texture with subsequent effects on organoleptic properties. Higher acceptability of pasta fortification with pumpkin flour could be due to the high content of protein. The conclusions drawn from this experiment are consistent with the one reported earlier by (Moh et al. 1999).

Texture profile analysis

Hardness

The most important textural attributes of cooked pasta are hardness. Major changes in the structure occur while cooking pasta, such as starch gelatinization and protein coagulation. For this, the texture of the final product gets affected. When the good quality pasta is cooked, during its initial stages, proteins absorb more water and swell faster than starch. Hydration of the protein fraction of pasta before the onset of starch gelatinization appears to play an important role in yielding a firm, high-quality pasta (Pritwani and Mathur 2017b). The first peak of the Texture Profile Analysis curve also showed a decline in its slope value for all samples with an increase in cooking time. The other reason is that the structure inside the uncooked pasta is effective for textural parameters. Cooking pasta exposes the surface to a much harsher heat. This will then change the conformational structure of the protein-starch network, causing loss or rigidity in its structure (Deák et al. 2015). Hardness results indicated that the interaction between cooking time and pasta type under cooking was significant ($p<0.05$). From the graph

1, it can be seen that the hardness of the sample cooked at 5 minutes was high compared to other time values of pasta samples in the same group.

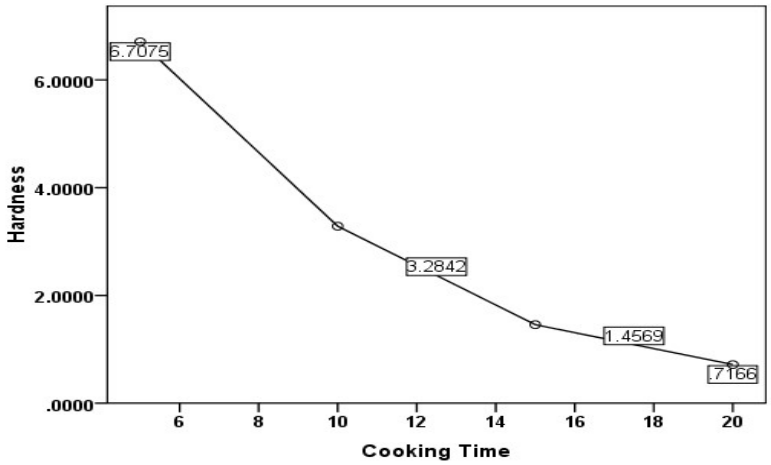

Graph 1: Hardness Estimation for Pasta Sample at Different Cooking Times

Chewiness

With cooking time, the chewiness for all pasta species decreased significantly because of the breakage of the gluten network and the loss of starch into the cooking water. Raw pasta is rather uniform in its structure while its cooked counterpart has a structure that is constantly changing from the surface to the core. The changes occur most greatly in the surface layer which has been subjected to the effects of cooking for the longest time period mentioned in Graph 2. There was a small amount of ungelatinized starch located in the center of cooked pasta, but outside the core region the starch granules have been gelatinized and swollen but still intact. The gluten was still elastic enough that it can stretch to accommodate the swollen starch granules resulting in a structure which was very dense. Closer to the surface of the strand, granules were no longer intact and starch present as strands or amorphous structures surrounded with protein network.

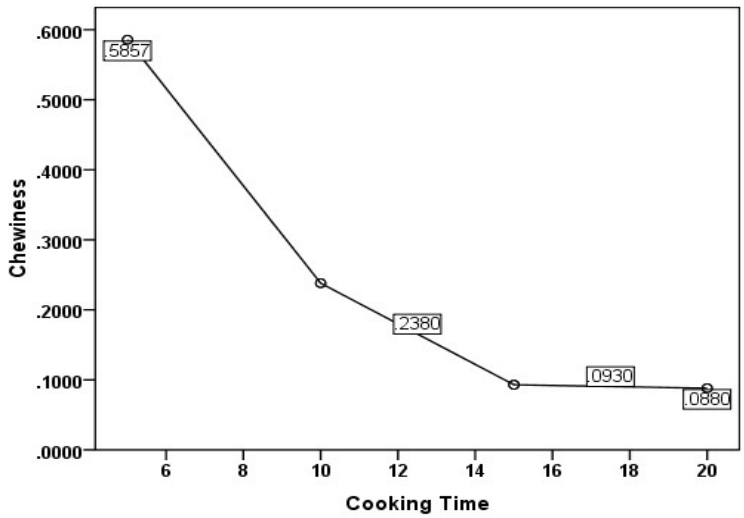

Graph 2: Chewiness Estimation for Pasta Sample at Different Cooking Times

Resilence

Resilience is the measure by which the sample recovers from deformation both in speed and forces derived. Resilience of cooked pasta was highly related with protein content(Nokkaew et al. 2019). Resilience values for the pasta samples were not significantly different from each other (Graph 3). Resilience values were found to be decreased by the cooking time changes from optimum to overcooked region as described in the figure. This causes pasta to become more plastic with increasing cooking time because of starch retrogradation and plasticization of polymeric chains by water action. Cooking time and type of pasta had significant effects on resilience during cooking ($P<0.05$).

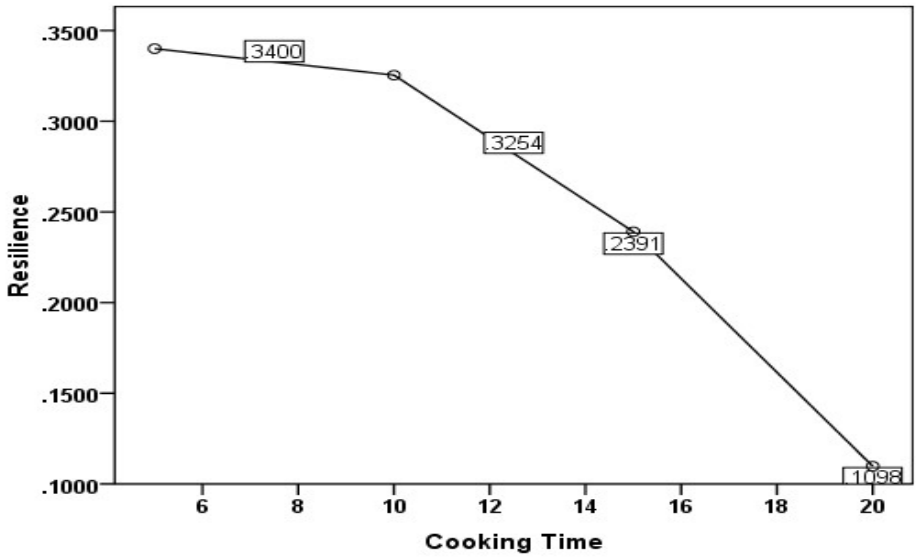

Graph 3: Resilience Estimation for Pasta Sample at Different Cooking Times

Springiness

While cooking increases springiness, it also increases represented in Graph 4. When there is an increase in the percentage of pumpkin flour the value decreases. Results of the Duncan multifactor variant: The effect of cooking time and pasta type on cohesiveness were significant ($P<0.05$).

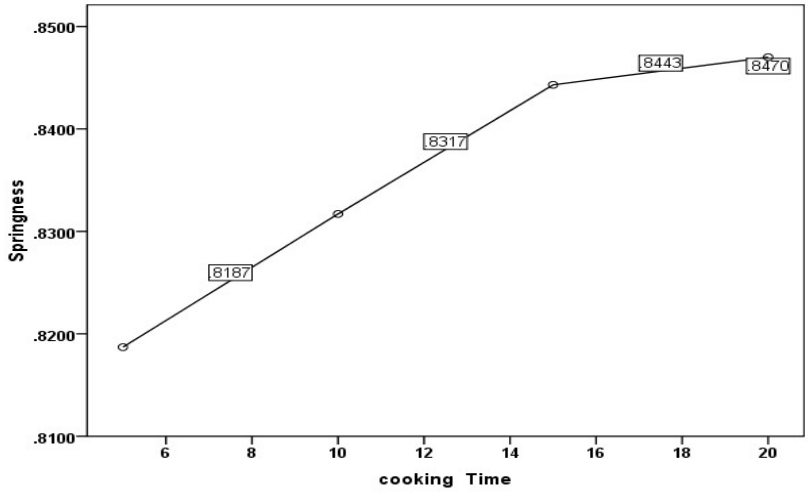

Graph 4: Springiness Estimation for pasta sample at Different Cooking Times

Cohesiveness

Coarse dependence of cohesiveness of pasta is dependent basically on the competition between the starch and protein molecules to form a continued network. Cohesiveness values, which are observed (Graph 5) to change more up to 10 min of cooking. Duncan multifactor variants results presented that the effect of cooking time and type of pasta on the cohesiveness was significant at $P<0.05$. Water may migrate from sites where it is bound more strongly into sites where it is weaker bound during cooking. Riva et al. (2000) stated that water is tighter bound to the proteins than starch. The diffusion of water into the starch granules is restricted by a protein network, and this is directly related to cohesiveness.

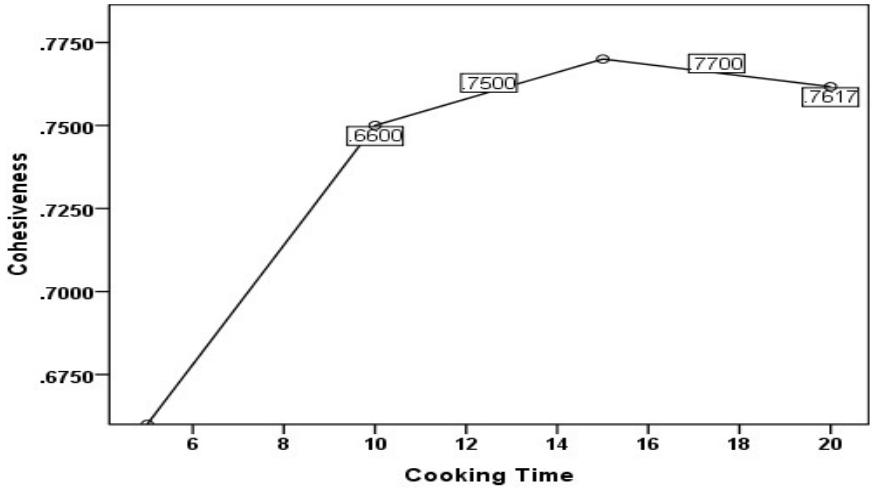

Graph 5: Cohesiveness Estimation for Pasta Sample at Different Cooking Times

Gumminess

As the cooking time increases the gumminess value is decreased (Graph 6). Duncan multi factor variate results showed that effect of cooking time and pasta type on gumminess was significant ($P<0.05$).

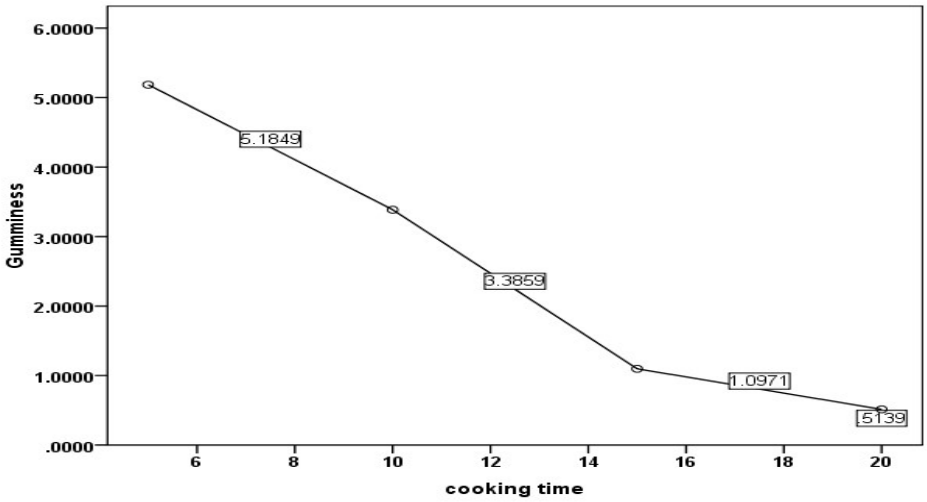

Graph 6: Gumminess Estimation for Pasta Sample at Different Cooking Times

IMAGE ANALYSIS

Cross sections of dry pasta made from different flours by scanning electron microscopy showed (Figure 9) differences in the binding forces between the protein matrix and starch granules. The cross-sectional sample preparation of durum wheat pasta by a blade showed higher strength of the binding force between the protein and starch, as opposed to that of soft wheat pasta prepared by a blade. These results coincided with those found by (Riyanto, Martono, and Rohman 2020).

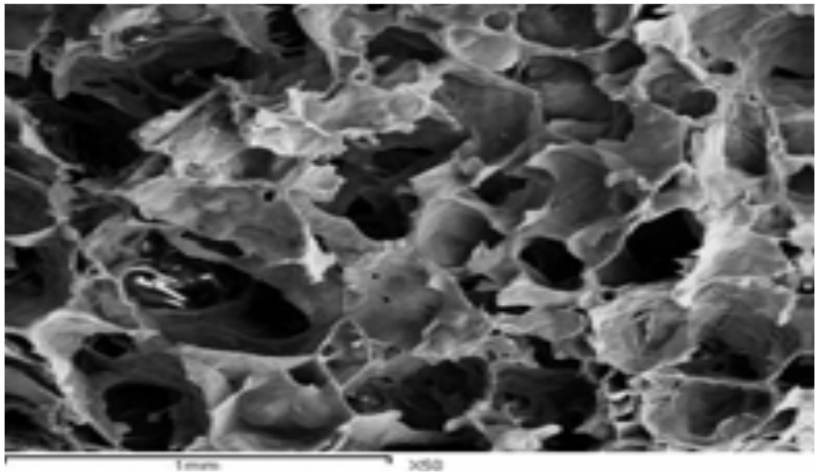

Figure 9: Image analysis for sample (pF) with15% pumpkin and oats flour

Microbial Analysis:

Under storage conditions at 4°C (chiller), no microorganisms were observed, and no counts were recorded during the 45-day testing period of samples. Similarly, under ambient conditions, no microorganisms were detected, and counts remained absent throughout the 45-day testing period. However, upon opening the storage container, shelf life was observed to decrease, leading to the formation of microorganisms.

Total Plate Count:

To determine the plate count, the following procedure was employed: From each dilution, 0.1 ml was added in duplicate to the plates containing plate count agar, and then spread using a sterile spreader (spread plate method). Subsequently, the plates were incubated at 37°C for 48

hours, and the colonies were counted. The colony counts were then calculated and expressed as log CFU per gram of the sample. Alternatively, 1 ml of each dilution was added in duplicate to sterile Petri plates containing sterile plate count agar, which was cooled to 45°C. The mixture was thoroughly mixed, and the media allowed to solidify before incubation and subsequent colony counting (pour plate method).

Detection of Enterobacteriaceae:
To determine the presence of Enterobacteriaceae, the following procedure was implemented: Buffered peptone water was utilized to incubate the test portion at 37°C for a period of 18 hours, with an additional 2 hours. Following this, the enrichment broth (EE broth) was inoculated with culture obtained from the pre-enrichment stage. Violet red bile glucose agar, serving as a selective media, was then inoculated with culture from the enrichment. The plates were subsequently incubated at 37°C for 24 hours, with an additional 2 hours. The characteristic colonies observed were confirmed by assessing fermentation of glucose and the presence of oxidase.

Total coliform:
To ascertain the coliform count, the following procedure was employed: The number of coliform bacteria was determined using the most probable number technique (MPN method). From the initial three dilutions, 1 ml each was added into five tubes (for each dilution) of Brilliant green lactose bile broth. These tubes were then incubated at 37°C for a duration of 48 hours. Turbidity and gas formation (collected in Durham's tubes within the media) were observed. The count of positive tubes was recorded, and the counts in the original sample were enumerated.

PROTEIN AND LIGAND PREPARATION

4.7.1 PROTEIN PREPARATION

The 3D structure Wild-Type Human Pancreatic Alpha-Amylase (*4X9Y)* & Human Aldose Reductase in complex with ALR25 *(6TUC)* were retrieved from protein data bank.

Figure 11: Human Alpha-Amylase (*4X9Y)*

Figure 11: Human Aldose *(6TUC)*

4.7.2 LIGAND PREPARATION

The ligand structures of 22 compounds were downloaded from PubChem.

Table 4: GC-MS result of Pumpkin powder

Sl.No:	Compound Name	Molecular formula	Molecular weight (g/mol)	
1	Vit E	$C_{29}H_{50}O_2$	430.7	14985
2	(5aR,6S,8S,10S,11S,11aS,12aR,13R)-5-methyl-5a,6,8,9,10,11,11a,12-octahydro-5H-6,10:11,12a-dimethanoindolo[3,2-b]quinolizine-8,13-diol	$C_{20}H_{26}N_2O_2$	326.4	441080
3	1H-imidazole, 2-ethyl-4-methyl	$C_6H_{1O}N_2$	110.16	70262
4	Methoxyphenamine	$C_{11}H_{17}NO$	179.26	4117
5	1,2-dihydroxyethyl-3,4-dihydroxyfuran-2(5H)-one	$C_6H_8O_6$	176.12	54670067
6	5-[1-hydroxy-2-(isopropylamino)ethyl]benzene-1,3-diol	$C_{11}H_{17}NO_3$	211.26	4086
7	2-Amino-9-[3,4-dihydroxy-5-(hydroxymethyl)oxolan-2-yl]-3H-purine-6-	$C_{10}H_{13}N_5O_5$	283.24	135402034
8	4,4'-methylenebis(tetrahydro-1,2H,4-thiadiazine)1,1,1',1'-tetraoxide	$C_7H_{16}N_4O_4S_2$	284.4	29566
9	3,7,11-trimethyl-2,6,10-dodecantrien-1-ol	$C_{15}H_{26}O$	222.37	3327
10	Tetradecanoic acid	$C_{14}H_{28}O_2$	228.37	11005
11	Squalene	$C_{30}H_{50}$	410.7	638072
12	3,7,11,15-tetramethyl-2-hexadecan-1-ol	$C_{20}H_{40}O$	296.5	5280435
13	1H-Purine-2, 6-dione, 3,7-dihydro-1,3- dimethyl-	$C_7H_8N_4O_2$	180.16	2153
14	1-β-D-ribofuranosyl-1H-1,2,4trazole-3-carboxamide	$C_8H_{12}N_4O_5$	244.2	9444
15	6,7-dimethoxy-3-[(5R)-4-methoxy-6-methyl-7,8-dihydro-5H-[1,3]dioxolo[4.5-g]isoquinolin-5-yl]-3H-2-benzofuran-1-on	$C_{22}H_{23}NO_7$	413.4	275196
16	1-(4-tert-butylphenyl)-4-[4-[hydroxyl(diphenyl)methyl]piperidin-1- yl]butan-1-ol	$C_{32}H_{41}NO_2$	471.7	5405
17	2-phenylethyl hydrazine	$C_8H_{12}N_2$	136.79	3675
18	2,6-di(propan-2-yl)phenyl	$C_{12}H_{18}O$	178.27	4943
19	4-[3-(5H-Dibenz[b,f]azepin-5-yl)-1-piperazinethanol	$C_{23}H_{29}N_3O$	363.5	10248163

20	5-fluoro-1-[4-hydroxy-5-(hydroxymethyl)tetrahydrofuran-2-yl]-1Hpyrimidine-2,4-dio	$C_9H_{11}FN_2O_5$	246.19	5790
21	4-chloro-N-(2-methyl-2,3-dihydroindol-1-yl)-3-sulfamoyl-benzamide	$C_{16}H_{16}clN_3O_3S$	365.8	3702
22	10,13-dimethylspiro[2,8,9,11,12,14,15,16-octahydro-1H-cyclopenta[a]phenanthrene-17,5'-oxolane]2',3-dione	$C_{22}H_{28}O_3$	340.5	319260

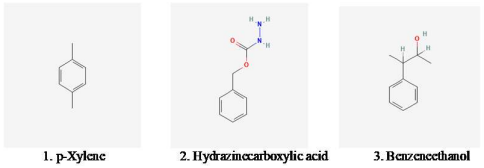
1. p-Xylene 2. Hydrazinecarboxylic acid 3. Benzeneethanol

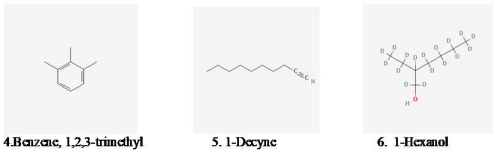
4.Benzene, 1,2,3-trimethyl 5. 1-Decyne 6. 1-Hexanol

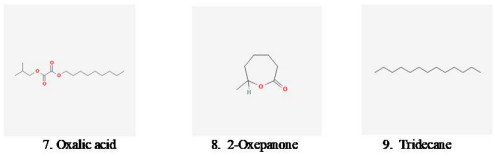
7. Oxalic acid 8. 2-Oxepanone 9. Tridecane

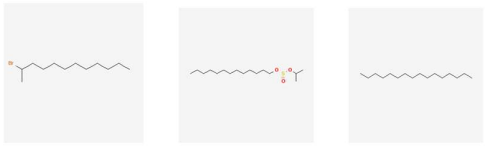
10. 2-Bromo dodecane 11. Sulfurous acid 12. Hexadecane


13.Vinyl 10-undecenoate 14. 1-Hexadecanol 15. Hexadecanoic acid


16. n-Hexadecanoic acid 17. Tritetracontane 18. i-Propyl 14-methyl-pentadecanoate

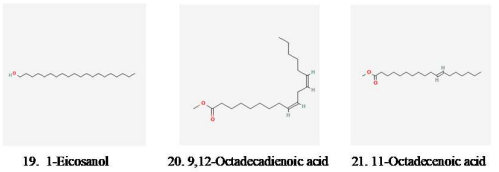
19. 1-Eicosanol 20. 9,12-Octadecadienoic acid 21. 11-Octadecenoic acid

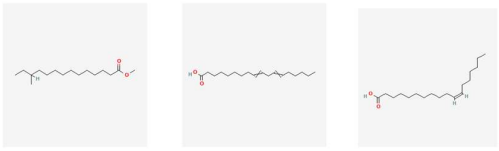
22. Tetradecanoic acid 23. 9,12-Octadecadienoic acid (Z, Z) 24. cis-Vaccenic acid

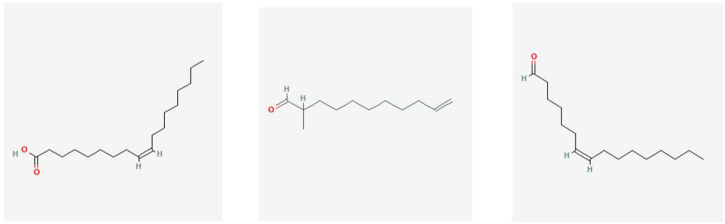
25. Oleic acid 26. 10-Undecen-1-al 27. 7-Hexadecenal, (Z)

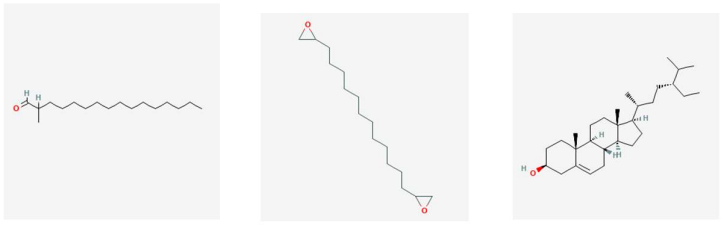
28. Hexadecanal 29. 1,2-15,16-Diepoxyhexadecane 30. Beta-sitosterol

Figure 12: 2D Structure of ligands

4.8 ACTIVE SITE IDENTIFICATION

The active site of *E. coli, Salmonella, Pseudomonas a*nd LDL receptor related protein which was used for docking study was identified using CASTp server. *E. coli, Salmonella, Pseudomonas* and LDL receptor related protein were selected and studied for the ligand interaction. The selected inhibitor compound molecules are interacting with various positions. The amino acid residues that were commonly involved in interaction with all the inhibitor molecules and the active pocket of *E. coli, Salmonella, Pseudomonas* and LDL receptor related protein were considered to be the domain containing following residues.

Active sites were identified using CASTp server.

1AJ0(ECOLI)

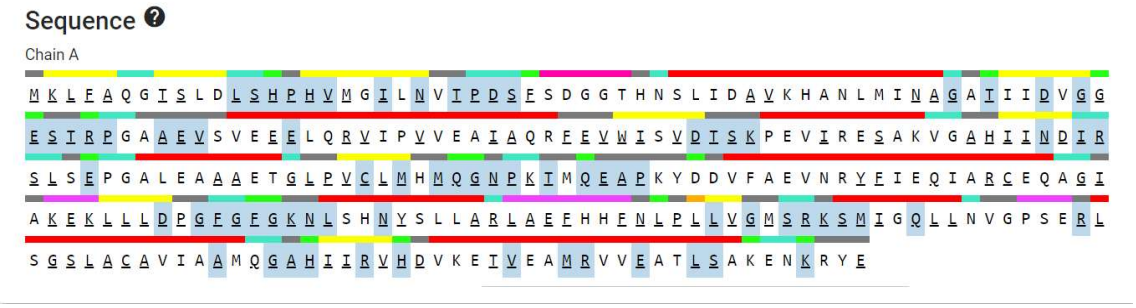

Figure 13: Active sites of *E.coli*

1X6X (PSE)

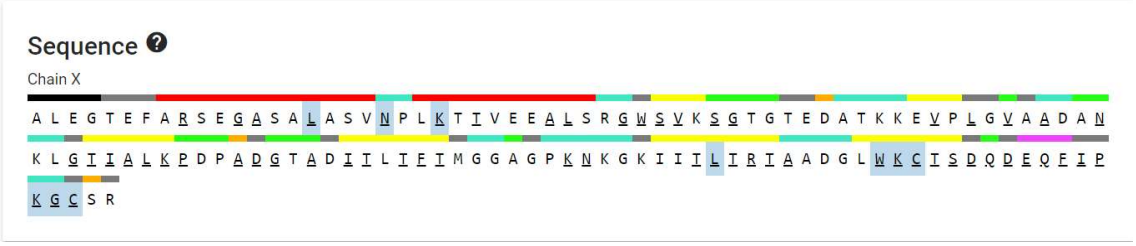

Figure 14: Active sites of *Pseudomonas*

4A0P

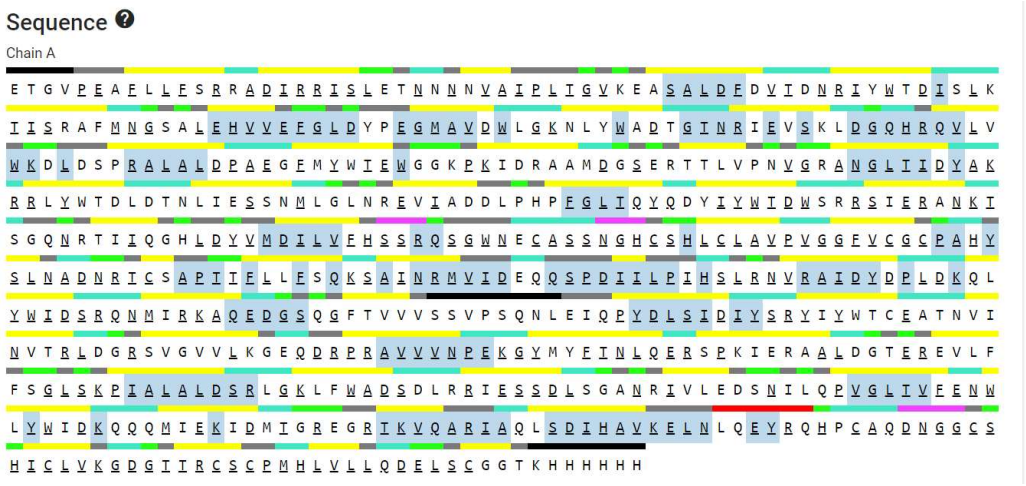

Figure 15: Active sites of LDL receptor related protein

4.9 RAMACHANDRAN PLOT OF *E. COLI, SALMONELLA, PSEUDOMONAS* AND LDL RECEPTOR RELATED PROTEIN

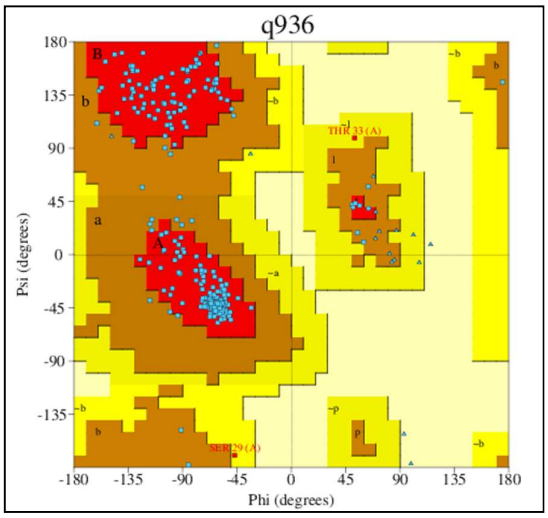

Figure 16: *E. coli*

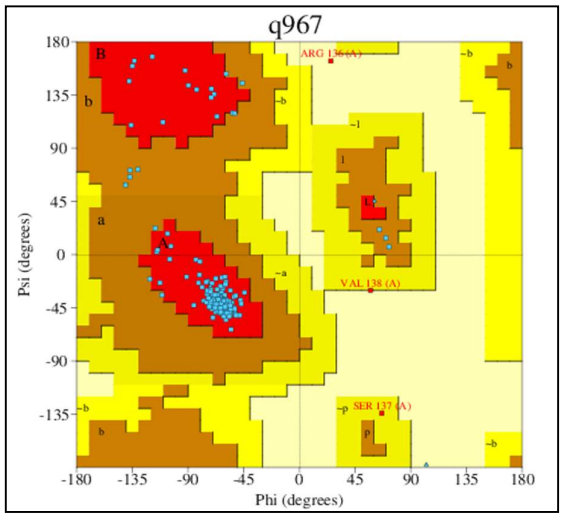

Figure 17: *Salmonella*

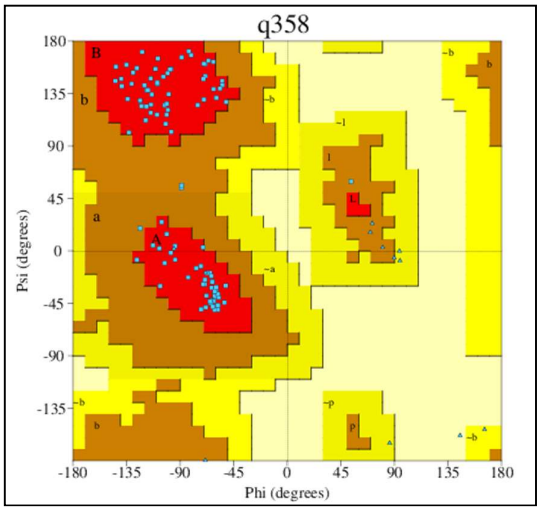

Figure 18: *Pseudomonas*

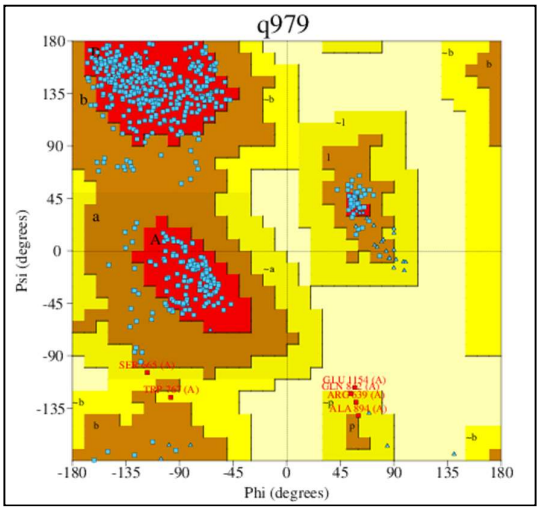

Figure 19: LDL receptor related protein

Table 6: Ramachandran Plot statistics for *E.Coli*

	No. of residues	**%-target**
Most favoured regions [A,B,L]	223	90.3%
Additional allowed regions [a,b,l,p]	22	8.9%
Generously allowed regions [~a,~b,~l,~p]	2	0.8%
Disallowed regions [XX]	0	0.0%
Non-glycine and non-proline residues	247	100.0%
End-residues (excl. Gly and Pro)	2	
Glycine residues	21	
Proline residues	12	
Total number of residues	282	

90% of the amino acid base pairs are fixed in the most favoured regions.

Table 7: Ramachandran Plot statistics for *Salmonella*

	No. of residues	**%-tage**
Most favoured regions [A,B,L]	154	90.1%
Additional allowed regions [a,b,l,p]	14	8.2%
Generously allowed regions [~a,~b,~l,~p]	1	0.6%

Disallowed regions [XX]	2	1.2%
Non-glycine and non-proline residues	171	100.0%
End-residues (excl. Gly and Pro)	2	
Glycine residues	8	
Proline residues	3	
Total number of residues	184	

90% of the amino acid base pairs are fixed in the most favoured regions.

Table 8: Ramachandran Plot statistics for *Pseudomonas*

	No. of residues	**%-tage**
Most favoured regions [A,B,L]	95	96.0%
Additional allowed regions [a,b,l,p]	4	4.0%
Generously allowed regions [~a,~b,~l,~p]	0	0.0%
Disallowed regions [XX]	0	0.0%
Non-glycine and non-proline residues	99	100.0%
End-residues (excl. Gly and Pro)	1	
Glycine residues	14	
Proline residues	6	
Total number of residues	120	

96% of the amino acid base pairs are fixed in the most favoured regions.

Table 9: Ramachandran Plot statistics for LDL receptor related protein

	No. of residues	**%-tage**
Most favoured regions [A,B,L]	460	84.9%
Additional allowed regions [a,b,l,p]	76	14.0%
Generously allowed regions [~a,~b,~l,~p]	5	0.9%
Disallowed regions [XX]	1	0.2%
Non-glycine and non-proline residues	542	100.0%

End-residues (excl. Gly and Pro)	3	
Glycine residues	41	
Proline residues	23	
Total number of residues	609	

85% of the amino acid base pairs are fixed in the most favoured regions.

4.10 PHARMACOLOGICAL PROPERTIES

Druglikeness and ADMET properties of shortlisted 32compounds were studied using SWISS ADME and ADMETsar server.

4.10.1 DRUGLIKENESS:

Results on drug similarity parameters of 30 compounds are shown in the table above. All drug-likeness data were within a substantial range indicating good drug-like behavior of the phytochemicals examined. Molecular LogP, MW and PSA showed good membrane permeability, intestinal absorption and oral bioavailability, while other parameters such as nHBA, nHBD and nRotb binding facilitate drug metabolism. and pharmacokinetics.

Lipinski's Rule of Five provides guidance on the solubility, bioavailability, and permeability of the drug molecule of interest

- molecular weight (acceptable range: ≤500)
- number of hydrogen bond donors (acceptable range: ≤5)
- number of hydrogen bond acceptors (acceptable range: ≤10)
- lipophilicity (expressed as LogP, acceptable range: <5)
- molar refractivity (40-130)
- A lower log P indicates that the drug molecule inside the cell is better absorbed. Log S values represent solubility and lower values again reflect better solubility. TPSA or Topological Polarized Surface is again associated with the absorption and permeability of drug molecule. Any candidate with a higher TSPA value generally results in poor permeability in the biological system.

Table 10: Drug-likeness properties of 30 compounds

Drug likeness property	**Molecular weight**	**Log P**	**Log S**	**H-Bond acceptor**	**H-Bond Donor**	**Molar refractivity**	**Heavy atoms**	**TPSA**	**Rotatable Bonds**
p-Xylene	106	2.12	-3.04	0	0	36.37	8	0.00 A^2	0
Hydrazinecarboxylic acid	166	1.54	-1.56	3	2	43.4	12	64.35 A^2	4

Benzeneethanol	150	2.17	-2.47	1	1	46.99	11	20.23 A²	2
Benzene, 1,2,3-trimethyl	120	2.22	-3.38	0	0	41.34	9	0.00 A²	0
1-Decyne	138	3.16	-3.19	0	0	48.35	10	0.00 A²	6
1-Hexanol	130	2.5	-2.26	1	1	41.73	9	20.23 A²	5
Oxalic acid	272	4.08	-4.26	4	0	76.79	19	52.6 A²	13
2-Oxepanone	128	1.77	-1.47	2	0	34.93	9	26.3 A²	0
Tridecane	184	4.03	-4.52	0	0	64.6	13	0.00 A²	10
2-Bromo dodecane	249	3.92	-4.89	0	0	67.67	13	0.00 A²	9
Sulfurous acid	306	4.53	-5.24	3	0	89.47	20	54.74 A²	15
Hexadecane	226	4.67	-5.6	0	0	79.03	16	0.00 A²	13
Vinyl 10-undecenoate	210	3.54	-3.37	2	0	64.94	15	26.30 A²	11
1-Hexadecanol	242	4.41	-4.9	1	1	80.19	17	20.23 A²	14
Hexadecanoic acid	256	3.85	-5.02	2	1	80.8	18	37.30 A²	14
n-Hexadecanoic acid	256	3.85	-5.02	2	1	80.8	18	37.30 A²	14

Tritetracontane	605	11.07	-15.39	0	0	208.82	43	0.00 A²	40
i-Propyl 14-methyl-pentadecanoate	298	5.06	-5.71	2	0	94.73	21	26.30 A²	15
1-Eicosanol	298	5.31	-6.35	1	1	99.42	21	20.23 Å²	18
9,12-Octadecadienoic acid	294	4.61	-4.97	2	0	93.78	21	26.30 Å²	15
11-Octadecenoic acid	296	4.79	-5.32	2	0	94.26	21	26.30 Å²	16
Tetradecanoic acid	256	4.08	-4.82	2	0	80.31	18	26.30 Å²	13
9,12-Octadecadienoic acid (Z, Z)	280	4.14	-5.05	2	1	89.46	20	37.30 Å²	14
cis-Vaccenic acid	282	4.12	-5.41	2	1	89.94	20	37.30 Å²	15
Oleic acid	282	4.27	-5.41	2	1	89.94	20	37.30 Å²	15
10-Undecen-1-al	182	3.02	-3.15	1	0	59.52	13	17.07 Å²	9
7-Hexadecenal, (Z)	238	3.91	-4.32	1	0	78.75	17	17.07 Å²	13
Hexadecanal	254	4.35	-5.29	1	0	84.03	18	17.07 Å²	14
1,2-15,16-Diepoxyhexadecane	254	4.29	-3.94	2	0	76.97	18	25.06 Å²	13
Beta-sitosterol	414	4.79	-7.9	1	1	133.23	30	20.23 Å²	6

4.10.2 ADMET PROPERTIES:

Table11: ADME/T properties of 30 compounds

The pharmacokinetics and toxicity, as well as other drug-like properties, of selected important phytochemicals were evaluated to assess efficacy and safety. In addition, some of the active properties of these key phytochemicals include carcinogenicity, hepatotoxicity, inhibition of p-glycoprotein, and inhibition of cytochrome P450 (CYP) and central nervous system (CNS) permeability, has been evaluated. Here, CNS permeability refers to the ability of a compound to selectively cross the blood-brain barrier. It has been shown that the osmotic value of the CNS must be greater than -2 to enter the CNS. No toxicity or carcinogenic potential remained in the selected phytochemicals.

4.11 MOLECULAR DOCKING ANALYSIS

4.11.1 DOCKING ANALYSIS OF *E. COLI*

4.11.1.1 *E. coli* vs beta-sitosterol

Insilico docking analysis was carried out with the *E. coli* and beta-sitosterol. The best ligand pose was selected based on the lowest binding energy confirmation. Upon docking, beta-sitosterol interacts with the *E.coli* with binding energy of -8.76 kcal/mol, RMSD of 39.954 Å, Inhibition constant, KI of 377.30 nM and the hydrophobic interactions are LEU3 (3.17 Å), PHE4 (3.03 Å), ALA5 (3.36 Å), LEU134 (3.02 Å), PRO135 (3.74 Å) , GLU180 (3.13 Å), LYS181 (3.43 Å) and the salt bridge is MET1 (3.77 Å).

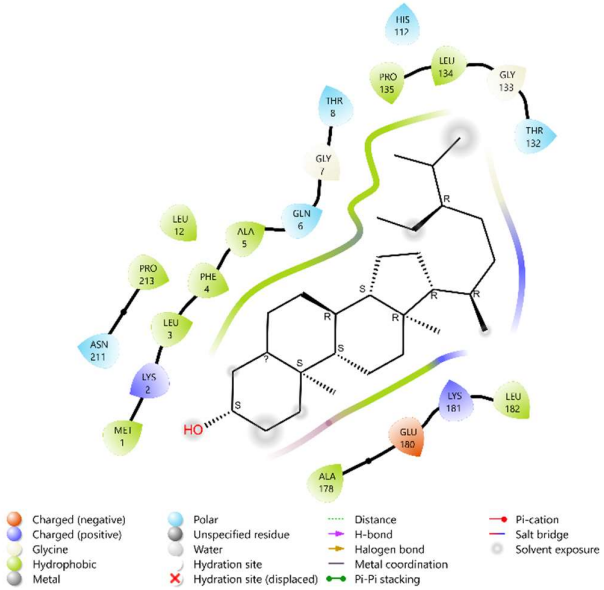

Figure 20a

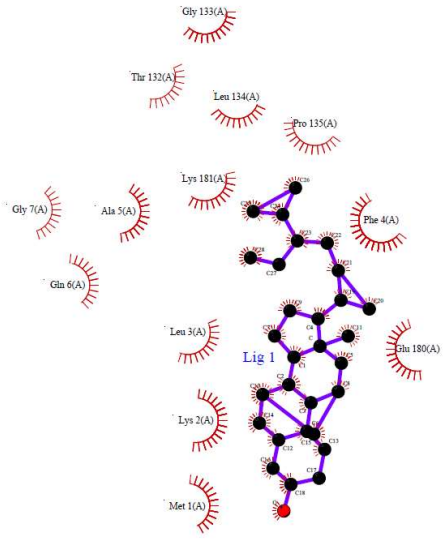

Figure 20b

Interaction between *E. coli* vs beta-sitosterol

4.11.1.2 *E.coli* vs 9,12-octadecadienoic acid (Z,Z)

Insilico docking analysis was carried out with the *E. coli* and 9,12-octadecadienoic acid (Z,Z). The best ligand pose was selected based on the lowest binding energy confirmation. Upon docking, 9,12-octadecadienoic acid (Z,Z) interacts with the *E.coli* with binding energy of -5.68

kcal/mol, RMSD of 38.071 Å, Inhibition constant, KI of 68.16 uM and the hydrophobic interactions are ARG63 (3.96 Å), PRO64 (3.38 Å), PHE190 (3.17 Å), PHE190 (3.79 Å) , ARG220 (3.62 Å), LYS221 (3.23 Å). The salt bridges are ARG63 (4.60 Å), ARG220 (4.03 Å) and HIS257 (4.65 Å).

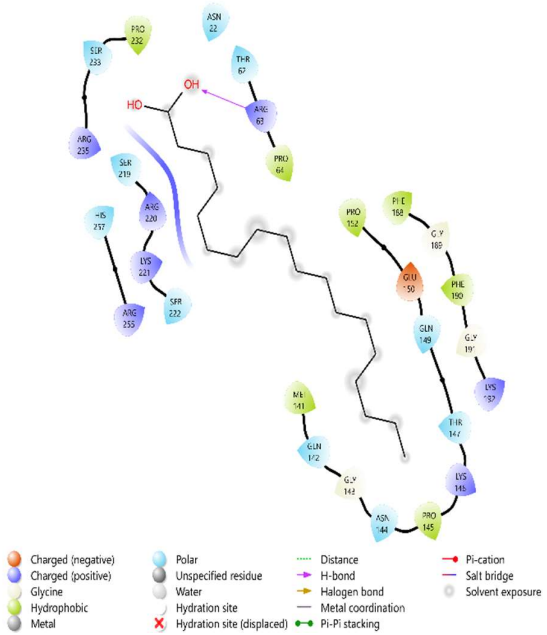

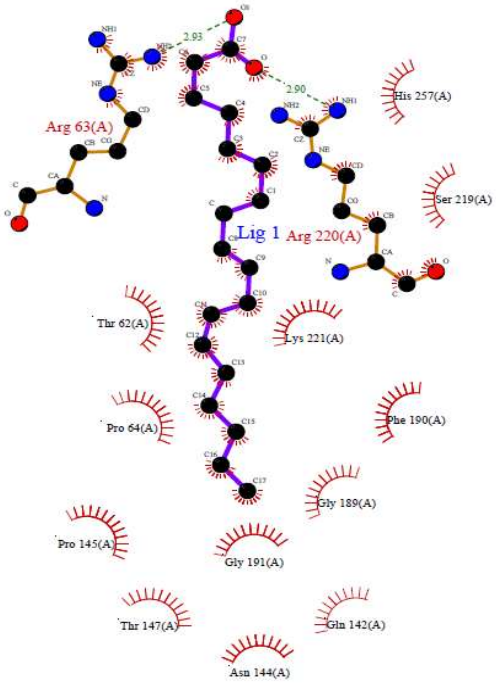

Figure 21a Figure 21b

Interaction between *E.coli* vs 9,12-octadecadienoic acid (Z,Z)

4.11.1.3 *E.coli* vs n-hexadecanoic acid

Insilico docking analysis was carried out with the *E.coli* and n-hexadecanoic acid . The best ligand pose was selected based on the lowest binding energy confirmation. Upon docking, n-hexadecanoic acid interacts with the *E.coli* with binding energy of -5.97 kcal/mol, RMSD of 38.149 Å, Inhibition constant, KI of 41.83 uM and the hydrophobic interactions are ARG63 (3.28 Å), PRO64 (3.30 Å), PHE190 (3.23 Å), PHE190 (3.63 Å) and the hydrogen bond is ASN22 (2.02 Å). The salt bridges are ARG63 (4.39 Å), ARG255 (4.53 Å) and HIS257 (4.31 Å).

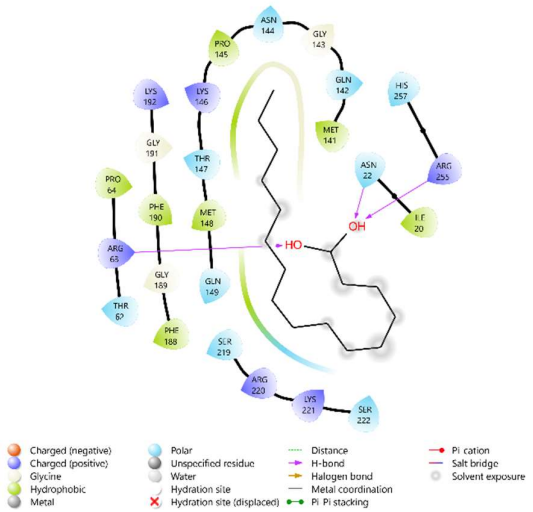

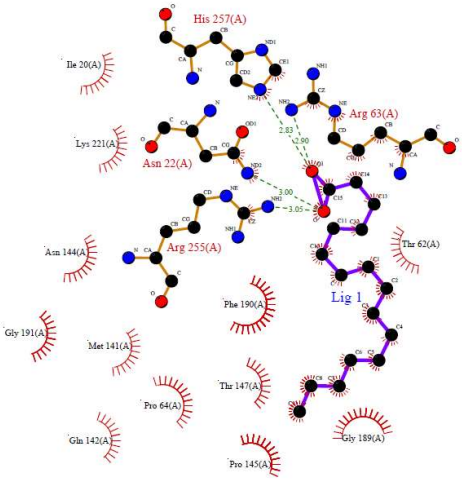

Figure 22a Figure 22b

Interaction between *E.coli* vs n-hexadecanoic acid

4.11.2 DOCKING ANALYSIS OF SALMONELLA

4.11.2.1 *Salmonella* vs beta-sitosterol

Insilico docking analysis was carried out with the *Salmonella* and beta-sitosterol. The best ligand pose was selected based on the lowest binding energy confirmation. Upon docking, beta-sitosterol interacts with the *Salmonella* with binding energy of -9.71 kcal/mol, RMSD of 37.545 Å, Inhibition constant, KI of 76.23 nM and the hydrophobic interactions are THR 85 (3.78 Å), ILE88 (3.09 Å), ILE88 (3.75 Å), TYR92 (3.39 Å), TYR92 (3.45 Å), LEU130 (3.40 Å), ARG136 (3.71 Å), LEU139 (3.79 Å), ASP152 (3.83 Å), PHE155 (3.54 Å), PHE155 (3.28 Å) and LEU156 (3.58 Å).

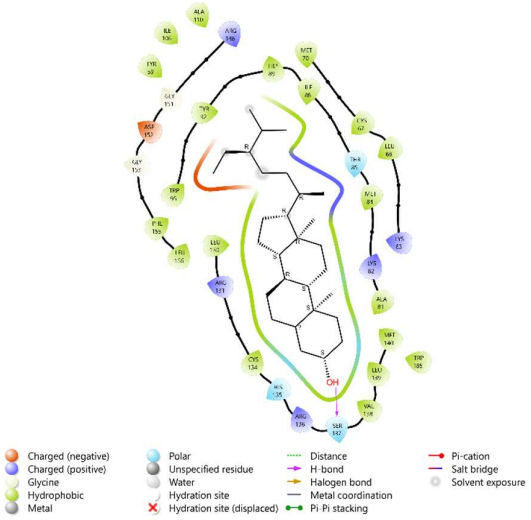

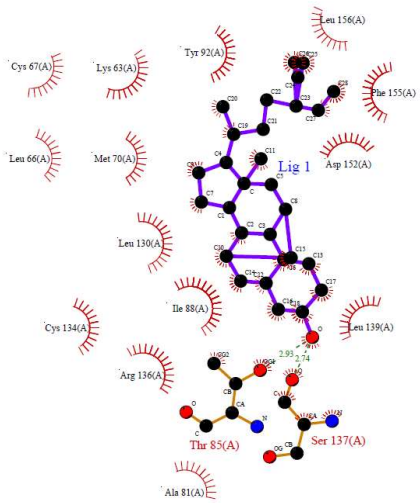

Figure 23a Figure 23b

Interaction between *Salmonella* vs beta-sitosterol

4.11.2.2 *Salmonella* vs 9,12-octadecadienoic acid (Z,Z)

Insilico docking analysis was carried out with the *Salmonella* and 9,12-octadecadienoic acid (Z,Z). The best ligand pose was selected based on the lowest binding energy confirmation. Upon docking, 9,12-octadecadienoic acid (Z,Z) interacts with the *Salmonella* with binding energy of -5.68 kcal/mol, RMSD of 36.541 Å, Inhibition constant, KI of 68.62 uM and the hydrophobic interactions are TYR59 (3.45 Å) , LYS63 (3.73 Å), LEU66 (3.38 Å), ILE88 (3.74 Å), TYR92 (3.47 Å), ILE106 (3.37 Å), LEU139 (3.69 Å), LEU139 (3.16 Å), ASP152 (3.67 Å), PHE155 (3.62 Å), PHE155 (3.06 Å), LEU156 (3.77 Å), LEU156 (3.29 Å) and the hydrogen bond is LEU139 (2.10 Å). The salt bridges are ARG136 (4.94 Å) and ARG148 (3.46 Å).

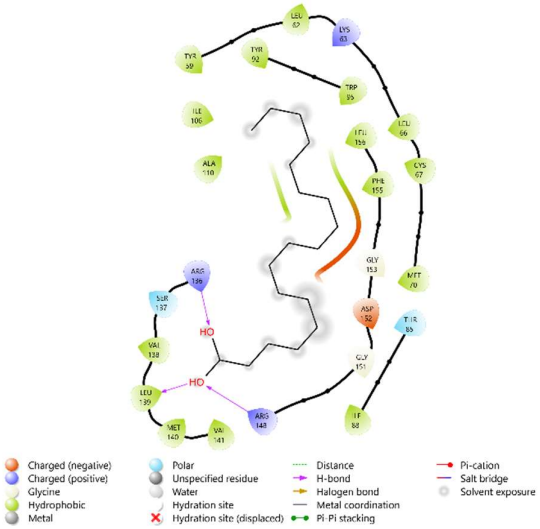

Figure 24a

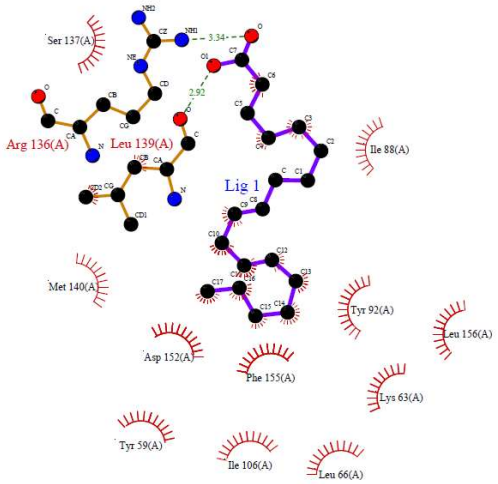

Figure 24b

Interaction between *Salmonella* vs 9,12-octadecadienoic acid (Z,Z)

4.11.2.3 *Salmonella* vs n-hexadecanoic acid

Insilico docking analysis was carried out with the *Salmonella* and n-hexadecanoic acid. The best ligand pose was selected based on the lowest binding energy confirmation. Upon docking, n-hexadecanoic acid interacts with the *Salmonella* with binding energy of -5.94 kcal/mol, RMSD of 22.496 Å, Inhibition constant, KI of 44.52 uM and the hydrophobic interactions are LYS10 (3.74 Å), GLN11 (3.20 Å), LEU14 (3.85 Å), LEU60 (3.07 Å), LEU60 (3.62 Å), LYS63 (3.44 Å), ALA123 (3.60 Å), PHE127 (3.19 Å), PHE127 (3.70 Å) and the hydrogen bonds are LYS10 (2.93 Å) and GLN11 (1.93 Å).

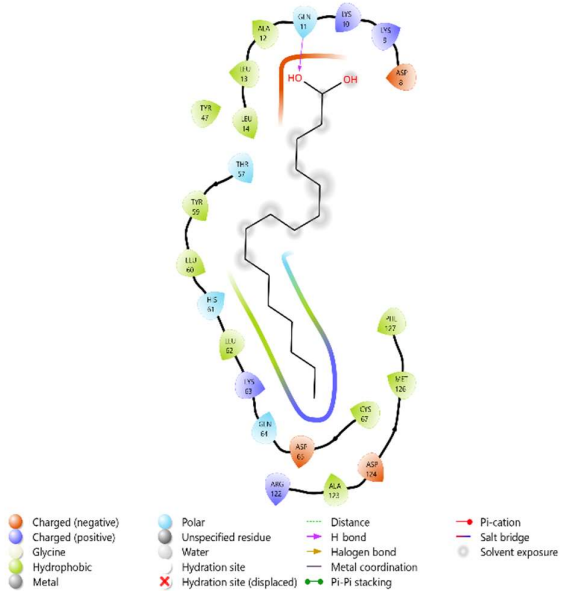

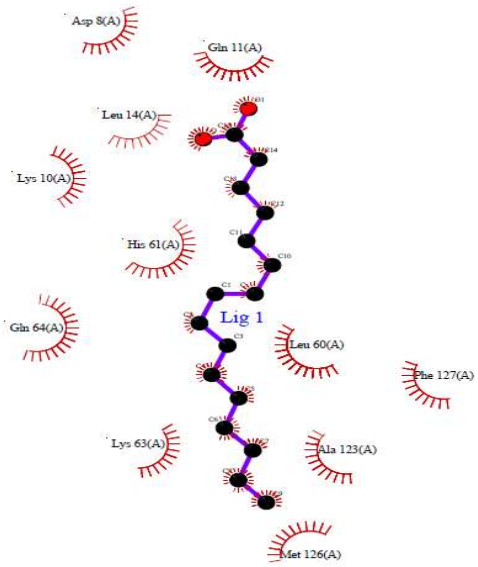

Figure 25a Figure 25b

Interaction between *Salmonella* vs n-hexadecanoic acid

4.11.3 DOCKING ANALYSIS OF PSEUDOMONAS

4.11.3.1 *Pseudomonas* vs beta-sitosterol

Insilico docking analysis was carried out with the *Pseudomonas* and beta-sitosterol. The best ligand pose was selected based on the lowest binding energy confirmation. Upon docking, beta-sitosterol interacts with the *Pseudomonas* with binding energy of -7.56 kcal/mol, RMSD of 58.097 Å, Inhibition constant, KI of 2.87 uM and the hydrophobic interactions are GLU32 (3.67 Å), LYS81 (3.38 Å), LEU82 (3.09 Å) and the hydrogen bond is LYS81 (3.01 Å).

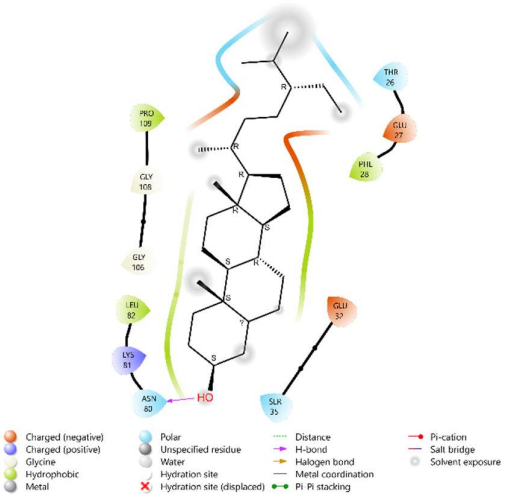

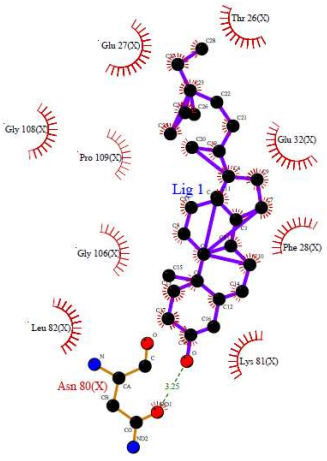

Figure 26a Figure 26b

Interaction between *Pseudomonas* vs beta-sitosterol

4.11.3.2 *Pseudomonas* vs 9,12-octadecadienoic acid (Z,Z)

Insilico docking analysis was carried out with the *Pseudomonas* and 9,12-octadecadienoic acid (Z,Z). The best ligand pose was selected based on the lowest binding energy confirmation. Upon docking, 9,12-octadecadienoic acid (Z,Z) interacts with the *Pseudomonas* with binding energy of -4.00 kcal/mol, RMSD of 51.216 Å, Inhibition constant, KI of 1.17 mM.

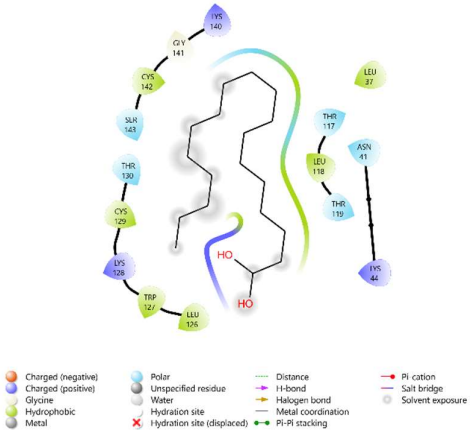

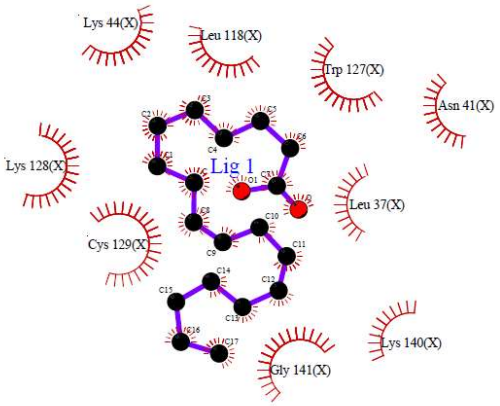

Figure 27a Figure 27b

Interaction between *Pseudomonas* vs 9,12-octadecadienoic acid (Z,Z)

4.11.3.3 *Pseudomonas* vs n-hexadecanoic acid

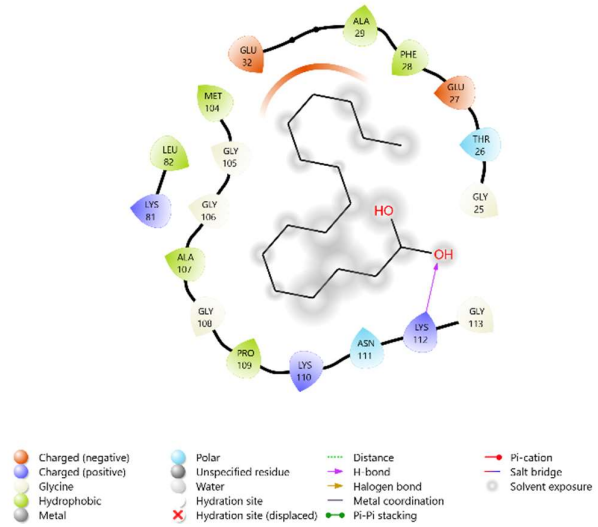

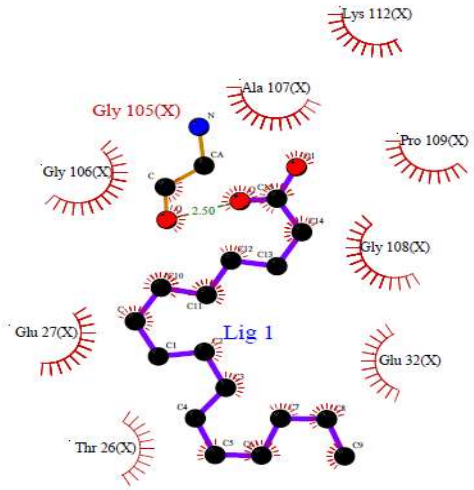

Figure 28a Figure 28b

Interaction between *Pseudomonas* vs n-hexadecanoic acid.

Insilico docking analysis was carried out with the *Pseudomonas* and n-hexadecanoic acid. The best ligand pose was selected based on the lowest binding energy confirmation. Upon docking, n-hexadecanoic acid interacts with the *Pseudomonas* with binding energy of -4.09 kcal/mol, RMSD of 58.692 Å, Inhibition constant, KI of 997.39 uM and the hydrophobic interaction is

PRO109 (3.82 Å) and the hydrogen bond is GLY105 (1.86 Å). The salt bridge is LYS112 (2.66 Å).

4.11.4 DOCKING ANALYSIS OF LDL RECEPTOR RELATED PROTEIN

4.10.4.1 LDL vs beta-sitosterol

Insilico docking analysis was carried out with the LDL and beta-sitosterol. The best ligand pose was selected based on the lowest binding energy confirmation. Upon docking, beta-sitosterol interacts with the LDL with binding energy of -10.11 kcal/mol, RMSD of 83.221 Å, Inhibition constant, KI of 39.16 nM and the hydrophobic interactions are GLU701 (3.71 Å), PHE702 (3.79 Å), ARG739 (3.37 Å), PRO917 (3.39 Å), ILE957 (3.44 Å), PRO960 (3.09 Å), ASP995 (3.32 Å). The hydrogen bonds are ALA918 (1.89 Å) and ARG946 (2.02 Å).

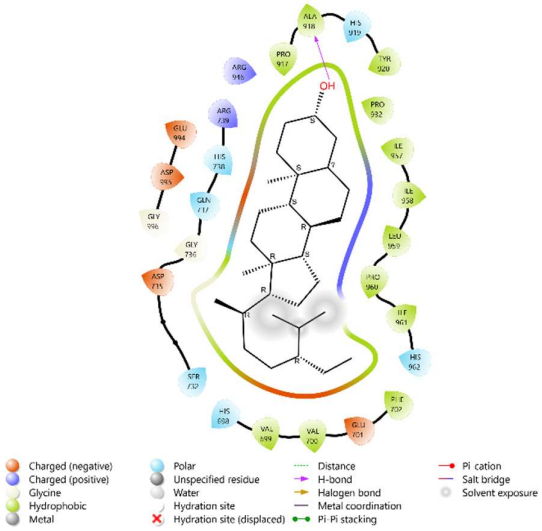

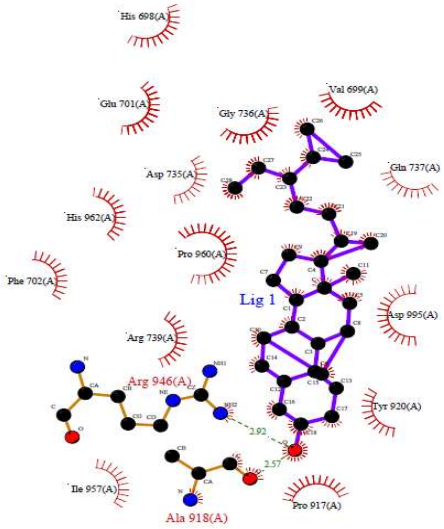

Figure 29a Figure 29b

Interaction between LDL vs beta-sitosterol

4.10.4.2 LDL vs 9,12-octadecadienoic acid (Z,Z)

Insilico docking analysis was carried out with the LDL and9,12-octadecadienoic acid (Z,Z). The best ligand pose was selected based on the lowest binding energy confirmation. Upon docking, 9,12-octadecadienoic acid (Z,Z) interacts with the LDL with binding energy of -5.53 kcal/mol, RMSD of 98.347 Å, Inhibition constant, KI of 87.69 uM and the hydrophobic interactions are ALA666 (3.88 Å), GLU708 (3.32 Å), ALA711 (3.39 Å), ARG751 (3.08 Å), ALA754 (3.78 Å), TRP767 (3.73 Å), PHE836 (3.49 Å), PHE836 (3.03 Å). The hydrogen bonds are ILE798 (2.03 Å), TYR800 (2.24 Å) and the salt bridge is ARG886 (4.74 Å).

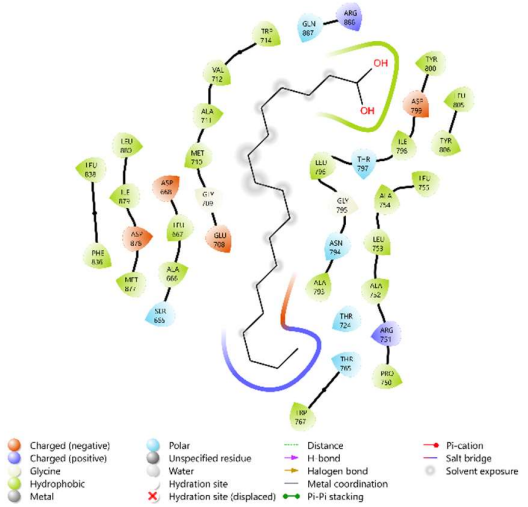

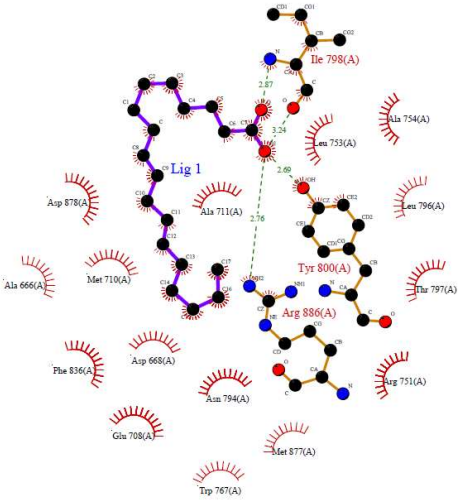

Figure 30a Figure 30b

Interaction between LDL vs 9,12-octadecadienoic acid (Z,Z)

4.10.4.3 LDL vs n-hexadecanoic acid

Insilico docking analysis was carried out with the LDL and n-hexadecenoic acid. The best ligand pose was selected based on the lowest binding energy confirmation. Upon docking, n-hexadecenoic acid interacts with the LDL with binding energy of -3.95 kcal/mol, RMSD of 83.041 Å, Inhibition constant, KI of 1.28 mM and the hydrophobic interactions are ARG739 (3.70 Å), PRO917 (3.91 Å), ILE957 (3.10 Å), PRO960 (3.71 Å). The hydrogen bonds are GLU701 (2.12 Å), PHE702 (2.22 Å) and the salt bridge is ARG739 (5.15 Å).

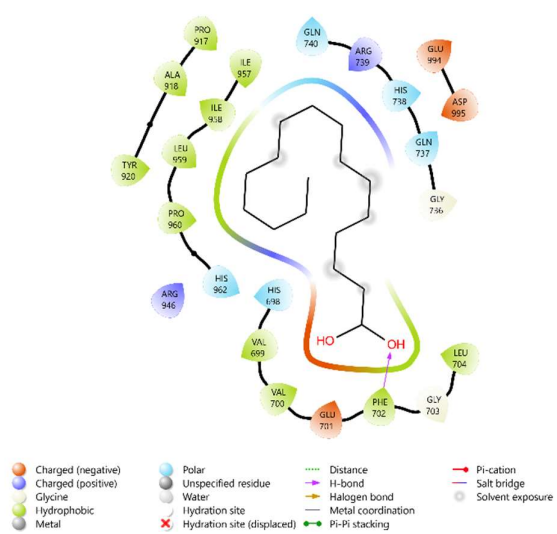

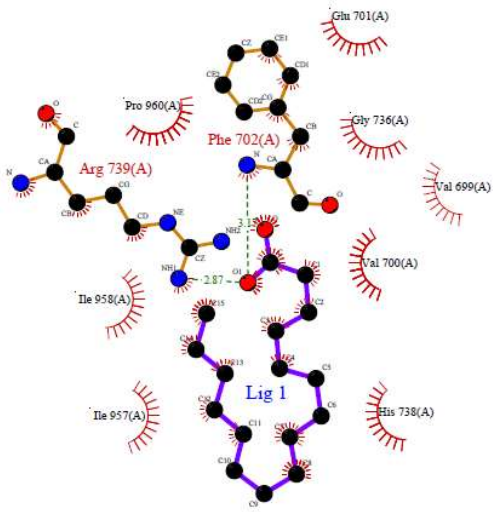

Figure 31a Figure 31b

Interaction between LDL vs n-hexadecanoic acid

Conclusion:

The study focused on the development and evaluation of pasta enriched with pumpkin and oat flour to enhance its nutritional and functional qualities and indicates that a formulation containing up to 10% pumpkin flour achieves optimal sensory acceptance and maintains desirable cooking and textural properties. The incorporation of pumpkin flour significantly increased the β-carotene and fiber content in pasta, adding to its health benefits. β-glucan levels also improved with the addition of oats, which is beneficial for heart health. However, the study identified an optimal pumpkin flour percentage, as higher levels could negatively impact taste and consumer preference. Pumpkin flour influenced the pasta's water absorption and cooking properties. Increasing pumpkin content reduced the optimum cooking time and cooking losses, which is advantageous for consumer convenience. However, it also increased the swelling index and cooking loss slightly, indicating changes in starch-protein interactions. Pasta samples with up to 15% pumpkin flour had acceptable sensory attributes, with a preference for the sample containing around 10% pumpkin flour. The obtained formulation of pasta is 15% of pumpkin flour with 85% of oats flour showing better sensory properties and nutritional properties. Although higher pumpkin flour content enhanced nutritional value, it affected taste and aroma, requiring further refinement for consumer acceptance. Pumpkin and oat flour modified the pasta's texture, reducing hardness and resilience. This change in texture could appeal to consumers looking for softer pasta options, though adjustments to the formulation might be necessary to achieve a balance between firmness and chewiness. The pasta samples demonstrated good microbial stability under refrigeration, with no growth detected over a 45-day period. This suggests that the enriched pasta could have a reasonable shelf life when stored properly, supporting its potential for commercial distribution. The findings underscore the potential of pumpkin and oat flour as valuable ingredients in functional pasta products, with implications for enhancing dietary intake of fiber and essential nutrients. Further research could optimize formulations to balance nutritional improvements with sensory attributes, ensuring consumer acceptability.

References:

Abdullah, S, Rama Chandra Pradhan, Muhammed Aflah, and Sabyasachi Mishra. 2020. "Efficiency of Tannase Enzyme for Degradation of Tannin from Cashew Apple Juice: Modeling and Optimization of Process Using Artificial Neural Network and Response Surface Methodology." *Journal of Food Process Engineering* 43 (10): e13499.

Abrha, Tesfalem, Yonas Girma, Kebede Haile, Mezgebe Hailu, and Mengistu Hailemariam. 2016. "Prevalence and Associated Factors of Clinical Manifestations of Vitamin a Deficiency among Preschool Children in Asgede-Tsimbla Rural District, North Ethiopia, a Community Based Cross Sectional Study." *Archives of Public Health* 74:1–8.

Agroindustriais, Produtos. 2013. "AOAC. Official Methods of Analysis of the Association of Official Analytical Chemists." *Caracterização, Propagação E Melhoramento Genético De Pitaya Comercial E Nativa Do Cerrado* 26 (74): 62.

Amin, M Ziaul, Tahera Islam, M Rasel Uddin, M Jashim Uddin, M Mashiar Rahman, and M Abdus Satter. 2019. "Comparative Study on Nutrient Contents in the Different Parts of Indigenous and Hybrid Varieties of Pumpkin (Cucurbita Maxima Linn.)." *Heliyon* 5 (9).

AOAC, Horwitz W. 2000. "International A: Official Methods of Analysis of the AOAC International." *The Association: Arlington County, VA, USA*.

Aremu, S O, and C C Nweze. 2017. “Determination of Vitamin A Content from Selected Nigerian Fruits Using Spectrophotometric Method.” *Bangladesh Journal of Scientific and Industrial Research* 52 (2): 153–58.

Asp, Nils G, Claes G Johansson, Haakan Hallmer, and Monica Siljestroem. 1983. “Rapid Enzymic Assay of Insoluble and Soluble Dietary Fiber.” *Journal of Agricultural and Food Chemistry* 31 (3): 476–82.

Bae, In Young, Sung Mi Kim, Suyong Lee, and Hyeon Gyu Lee. 2010. “Effect of Enzymatic Hydrolysis on Cholesterol-Lowering Activity of Oat β-Glucan.” *New Biotechnology* 27 (1): 85–88.

Baranska, Malgorzata, W Schütze, and Hartwig Schulz. 2006. “Determination of Lycopene and β-Carotene Content in Tomato Fruits and Related Products: Comparison of FT-Raman, ATR-IR, and NIR Spectroscopy.” *Analytical Chemistry* 78 (24): 8456–61.

Barba, A I Olives, M Cámara Hurtado, M C Sánchez Mata, V Fernández Ruiz, and M López Sáenz De Tejada. 2006a. “Application of a UV–Vis Detection-HPLC Method for a Rapid Determination of Lycopene and β-Carotene in Vegetables.” *Food Chemistry* 95 (2): 328–36.

———. 2006b. “Application of a UV–Vis Detection-HPLC Method for a Rapid Determination of Lycopene and β-Carotene in Vegetables.” *Food Chemistry* 95 (2): 328–36.

Biswas, A K, J Sahoo, and M K Chatli. 2011. “A Simple UV-Vis Spectrophotometric Method for Determination of β-Carotene Content in Raw Carrot, Sweet Potato and Supplemented Chicken Meat Nuggets.” *LWT-Food Science and Technology* 44 (8): 1809–13.

Braaten, J T, P J Wood, F W Scott, M S Wolynetz, M K Lowe, P Bradley-White, and M W Collins. 1994a. “Oat Beta-Glucan Reduces Blood Cholesterol Concentration in Hypercholesterolemic Subjects.” *European Journal of Clinical Nutrition* 48 (7): 465–74.

———. 1994b. “Oat Beta-Glucan Reduces Blood Cholesterol Concentration in Hypercholesterolemic Subjects.” *European Journal of Clinical Nutrition* 48 (7): 465–74.

Careri, Maria, Lisa Elviri, and Alessandro Mangia. 1999. “Liquid Chromatography–Electrospray Mass Spectrometry of β-Carotene and Xanthophylls: Validation of the Analytical Method.” *Journal of Chromatography A* 854 (1–2): 233–44.

Carvalho, Lucia Maria Jaeger de, Lara de Azevedo Sarmet Moreira Smiderle, José Luiz Viana de Carvalho, Flavio de Souza Neves Cardoso, and Maria Gabriela Bello Koblitz. 2014. “Assessment of Carotenoids in Pumpkins after Different Home Cooking Conditions.” *Food Science and Technology* 34:365–70.

Chen, Yulian, Yan Qiao, Y U Xiao, Haochun Chen, Liang Zhao, Ming Huang, and Guanghong Zhou. 2016. “Differences in Physicochemical and Nutritional Properties of Breast and Thigh Meat from Crossbred Chickens, Commercial Broilers, and Spent Hens.” *Asian-Australasian Journal of Animal Sciences* 29 (6): 855.

Cheng, Hsing-Hsien, and Ming-Hoang Lai. 2000. “Fermentation of Resistant Rice Starch Produces Propionate Reducing Serum and Hepatic Cholesterol in Rats.” *The Journal of Nutrition* 130 (8): 1991–95.

Deák, Konrád, Tamás Szigedi, Zoltán Pék, Piotr Baranowski, and Lajos Helyes. 2015. "Carotenoid Determination in Tomato Juice Using near Infrared Spectroscopy." *International Agrophysics* 29 (3).

Drozdowski, Laurie A, Raylene A Reimer, Feral Temelli, Rhonda C Bell, Thava Vasanthan, and Alan B R Thomson. 2010. "β-Glucan Extracts Inhibit the in Vitro Intestinal Uptake of Long-Chain Fatty Acids and Cholesterol and down-Regulate Genes Involved in Lipogenesis and Lipid Transport in Rats." *The Journal of Nutritional Biochemistry* 21 (8): 695–701.

Ganesan, P, K Rathnakumar, B A Nicy, and V Vijayarahavan. 2017. "Improvement of Nutritional Value of Extruded Snack Product by Incorporation of Blanched Dried Fish Powder from Sardine and Lizard Fish and Selection by Organoleptic Evaluation." *Journal of Entomology and Zoology Studies* 5 (6): 2552–54.

Hooda, Seema, J Jacques Matte, Thavaratnam Vasanthan, and Ruurd T Zijlstra. 2010. "Dietary Oat β-Glucan Reduces Peak Net Glucose Flux and Insulin Production and Modulates Plasma Incretin in Portal-Vein Catheterized Grower Pigs." *The Journal of Nutrition* 140 (9): 1564–69.

Hussain, Ashiq, Tusneem Kausar, Ahmad Din, Anjum Murtaza, Muhammad Abdullah Jamil, Saima Noreen, and Muhammad Azhar Iqbal. 2021. "Antioxidant and Antimicrobial Properties of Pumpkin (Cucurbita Maxima) Peel, Flesh and Seeds Powders." *Journal of Biology, Agriculture and Healthcare* 11 (6): 42–51.

Javeria, Sadaf, Tariq Masud, Shehla Sammi, Saima Tariq, Asma Sohail, S J Butt, Kashif Sarfraz Abbasi, and Sartaj Ali. 2013. "Comparative Study for the Extraction of B-Carotene in Different Vegetables." *Pakistan Journal of Nutrition, Faisalabad* 12 (11): 983–89.

Karnjanawipagul, P, W Nittayanuntawech, P Rojsanga, and L Suntornsuk. 2010. "Analysis of β-Carotene in Carrot by Spectrophotometry." *Mahidol University Journal of Pharmaceutical Science* 37 (8).

Kim, Mi Young, Eun Jin Kim, Young-Nam Kim, Changsun Choi, and Bog-Hieu Lee. 2012. "Comparison of the Chemical Compositions and Nutritive Values of Various Pumpkin (Cucurbitaceae) Species and Parts." *Nutrition Research and Practice* 6 (1): 21–27.

Kreck, Mirjam, Petra Kuerbel, Michael Ludwig, Peter J Paschold, and Helmut Dietrich. 2006. "Identification and Quantification of Carotenoids in Pumpkin Cultivars (Cucurbita Maxima L.) and Their Juices by Liquid Chromatography with Ultraviolet-Diode Array Detection."

Kris-Etherton, Penny M, William S Harris, and Lawrence J Appel. 2002. "Fish Consumption, Fish Oil, Omega-3 Fatty Acids, and Cardiovascular Disease." *Circulation* 106 (21): 2747–57.

Kwiri, Raphael, Clive Winini, Amos Musengi, Misheck Mudyiwa, Clarice Nyambi, Perkins Muredzi, and Abigail Malunga. 2014. "Proximate Composition of Pumpkin Gourd (Cucurbita Pepo) Seeds from Zimbabwe."

Moh, M H, Y B Che Man, B S Badlishah, S Jinap, M S Saad, and W J W Abdullah. 1999. "Quantitative Analysis of Palm Carotene Using Fourier Transform Infrared and near Infrared Spectroscopy." *Journal of the American Oil Chemists' Society* 76:249–54.

Nakazibwe, Immaculate, Eunice Apio Olet, and Grace Kagoro Rugunda. 2020. “Nutritional Physico-Chemical Composition of Pumpkin Pulp for Value Addition: Case of Selected Cultivars Grown in Uganda.”

Nardo, Thais De, Cecilia Shiroma-Kian, Yuwana Halim, David Francis, and Luis E Rodriguez-Saona. 2009. “Rapid and Simultaneous Determination of Lycopene and β-Carotene Contents in Tomato Juice by Infrared Spectroscopy.” *Journal of Agricultural and Food Chemistry* 57 (4): 1105–12.

Nisa, Khairun, and Ryka Marina Walanda. 2021. “Analysis of Beta-Carotene from Jongi (Dillenia Serrata Thunb.) as a Source of Vitamin A.” *World Journal of Advanced Research and Reviews* 10 (2): 184–90.

Nkhata, Smith Gilliard, and Emmanuel Owino Ayua. 2018. “Quality Attributes of Homemade Tomato Sauce Stored at Different Temperatures.” *African Journal of Food Science* 12 (5): 97–103.

Nokkaew, Rayakorn, Vittaya Punsuvon, Tetsuya Inagaki, and Satoru Tsuchikawa. 2019. “Determination of Carotenoids and Dobi Content in Crude Palm Oil by Spectroscopy Techniques: Comparison of Raman and FT-NIR Spectroscopy.” *GEOMATE Journal* 16 (55): 92–98.

Norshazila, Shahidan, Othman Rashidi, and J Irwandi. 2014. “Carotenoid Content in Different Locality of Pumpkin (Cucurbita Moschata) in Malaysia.” *International Journal of Pharmacy and Pharmaceutical Sciences* 6 (3): 29–32.

Petracci, Massimiliano, Samer Mudalal, Elena Babini, and Claudio Cavani. 2014. “Effect of White Striping on Chemical Composition and Nutritional Value of Chicken Breast Meat.” *Italian Journal of Animal Science* 13 (1): 3138.

Pongjanta, Jirapa, Angkana Naulbunrang, Siriporn Kawngdang, Tippawan Manon, and Thirawat Thepjaikat. 2006. “Utilization of Pumpkin Powder in Bakery Products.” *Songklanakarin Journal of Science and Technology* 28 (1): 71–79.

Prasetyo, Marisa, M Chia, C Hughey, and L M Were. 2008. “Utilization of Electron Beam Irradiated Almond Skin Powder as a Natural Antioxidant in Ground Top Round Beef.” *Journal of Food Science* 73 (1): T1–6.

Pritwani, R, and P Mathur. 2017a. “β-Carotene Content of Some Commonly Consumed Vegetables and Fruits Available in Delhi, India.” *J Nutr Food Sci* 7 (5): 1–7.

———. 2017b. “β-Carotene Content of Some Commonly Consumed Vegetables and Fruits Available in Delhi, India.” *J Nutr Food Sci* 7 (5): 1–7.

Quijano-Ortega, Natalia, Carlos Alberto Fuenmayor, Carlos Zuluaga-Dominguez, Consuelo Diaz-Moreno, Sanín Ortiz-Grisales, Maribel García-Mahecha, and Silvia Grassi. 2020. “FTIR-ATR Spectroscopy Combined with Multivariate Regression Modeling as a Preliminary Approach for Carotenoids Determination in Cucurbita Spp.” *Applied Sciences* 10 (11): 3722.

Riyanto, S Irnawati, S Martono, and A Rohman. 2020. “The Employment of FTIR Spectroscopy and Chemometrics for Authentication of Pumpkin Seed Oil from Sesame Oil.” *Food Research* 4 (1): 42–48.

Rungpichayapichet, Parika, Busarakorn Mahayothee, Pramote Khuwijitjaru, Marcus Nagle, and Joachim Müller. 2015. “Non-Destructive Determination of β-Carotene Content in

Mango by near-Infrared Spectroscopy Compared with Colorimetric Measurements." *Journal of Food Composition and Analysis* 38:32–41.

Skiepko, N, I Chwastowska-Siwiecka, J Kondratowicz, and D Mikulski. 2016. "The Effect of Lycopene Addition on the Chemical Composition, Sensory Attributes and Physicochemical Properties of Steamed and Grilled Turkey Breast." *Brazilian Journal of Poultry Science* 18:319–30.

Suknark, K, J Lee, R R Eitenmiller, and R D Phillips. 2001. "Stability of Tocopherols and Retinyl Palmitate in Snack Extrudates." *Journal of Food Science* 66 (6): 897–902.

Wood, PJ1, M U Beer, and G Butler. 2000. "Evaluation of Role of Concentration and Molecular Weight of Oat β-Glucan in Determining Effect of Viscosity on Plasma Glucose and Insulin Following an Oral Glucose Load." *British Journal of Nutrition* 84 (1): 19–23.

Zahra, Naseem, A Nisa, F Arshad, S M Malik, I Kalim, S Hina, A Javed, and S M Inam. 2016. "Comparative Study of Beta Carotene Determination by Various Methods: A Review." *Bio Bulletin* 2 (1): 96–106.